Dynamics of the Genesis heating rods

Coen Degen

Supervisors: Martin Rhode and Christian Marcel

Reactor Physics department
Faculty of Applied Sciences

TU Delft
10-05-2006

Contents

Abstract

In this report measurements and simulations are conducted to determine the heat transfer characteristics of the heating rods in the experimental Genesis setup. Measurements are done both in air and in Freon 134a. The first main result is the simulation of heat transfer through the Genesis heating rods and the acquisition of the time constants for the transfer function for a Genesis heating rod ($\tau_1 = 0,030\,\mathrm{s}$ and $\tau_2 = 0,28\,\mathrm{s}$). The numerical model is sufficiently verified by qualitative comparison to temperature measurements at the rod surface in air. Subsequently, simulations are conducted with a temperature dependent heat transfer coefficient for the Genesis geometry. The time constants associated with this process are found to be $\tau_1 = 0,12\,\mathrm{s}$ and $\tau_2 = 0.75\,\mathrm{s}$. It can be concluded that the transfer of heat from the rod surface to the coolant is slower than the transfer of heat within the rod and is, therefore, the limiting factor for the heat transfer. Also, attempts have been made to find a transfer function for the relation between input power and the pressure drop over the Genesis core, but an expression for such a transfer function could not be derived from the results generally due to data point shortage. Cross-correlation analysis shows that the total Genesis transfer function is made up of a fast component, associated to the rod, boundary layer and traveling time through the core, and a slow component, associated with the natural circulation. The values of the time constants of the combined rod and coolant transfer functions support this conclusion, as do the calculated traveling times for the core and the riser section. Due to these effects measurements turn out to be slower than the simulations.

A fourth order approximation for the total transfer function found in the literature, turns out to produce quite different results for the bode plots than those constructed from the measurements. This is most likely due to neglect of the natural circulation in the approximation.

1. Introduction

The Genesis facility is a scaled experimental setup of the Economic Simplified Boiling Water Reactor, designed by General Electric. For easy experimental access, the core is not heated by a fission process, but by electrically heated rods. To be sure the behavior of the Genesis facility to changing core conditions is similar to that of the ESBWR, we are very much interested in the transfer functions concerning the heat transfer from the heating rods to the coolant. An important question in this respect is if either the heat transfer through the rod or the heat transfer from the surface of the rod to the coolant is most important for the total heat transfer. For this purpose, measurements as well as numerical simulations of the heat transfer are conducted. After programming the simulations in Fortran 95, it has to be verified by experiments. If the model can be verified, we can determine, with the help of simulations of the heat transfer processes mentioned before, if one of them is the limiting factor for the total heat transfer. Moreover, measurements are done at the Genesis facility itself. The response to sinusoidal power input signals over a fixed frequency range is recorded to be used to determine the total Genesis transfer function $G_{dp,P}$. From this function we want to single out a description for the heat transfer from the surface of the rod to the surrounding Freon 134a boundary layer. This expression should then be independent of the characteristics of the heating rod. Finally, analyzing the total Genesis transfer function, qualitative descriptions of possible additional transfer functions incorporated in the measurements can be made. The experiments are conducted as a part of a Bachelor Project at the Physics of Nuclear Reactors group at Delft University of Technology.

2. Nomenclature

A list of symbols frequently used throughout the text. Unless indicated differently, the listed units are used.

a	thermal diffusivity ($\frac{\mathrm{W}}{\mathrm{m\,K}}$)
c_p	heat capacity ($\frac{\mathrm{J}}{\mathrm{kg\,K}}$)
D	characteristic length/diameter (m)
D_e	wetted diameter (m)
f	frequency (Hz)
G	general symbol used for transfer functions
G	mass flux in calculation $h_{2\Phi}$ ($\frac{\mathrm{kg}}{\mathrm{m^2\,s}}$)
h	heat transfer coefficient ($\frac{\mathrm{W}}{\mathrm{m^2\,K}}$)
i	numerical radius step indicator (number)
h_{cool}	heat transfer coefficient from Genesis rod cladding to coolant ($\frac{\mathrm{W}}{\mathrm{m^2\,K}}$)
h_{fg}	difference in heat transfer coefficient between the liquid and gaseous phase of the coolant ($\frac{\mathrm{W}}{\mathrm{m^2\,K}}$)
h_{NB}	nucleate boiling heat transfer coefficient ($\frac{\mathrm{W}}{\mathrm{m^2\,K}}$)
$h_{2\Phi}$	two phase boiling flow heat transfer coefficient ($\frac{\mathrm{W}}{\mathrm{m^2\,K}}$)
M	mass flow ($\frac{\mathrm{kg}}{\mathrm{s}}$)
p	pressure (Pa)
r	radius (m)
T	temperature (°C)
T_{sat}	mean temperature in boiling coolant (°C)
T_w	temperature at the rod surface (°C)
t	time (s)
$t_{core,2\Phi}$	void traveling time through the core (s)
t_{riser}	void travelling time through the riser (s)
$u(t)$	step function
U_{ab}	thermocouple potential difference (V)
V	volume ($\mathrm{m^3}$)

2. Nomenclature

v_0	core inlet velocity ($\frac{\mathrm{m}}{\mathrm{s}}$)
ΔW	distance between two consecutive windings (m)
x	quality
q'''	heat production per second per unit volume ($\frac{\mathrm{W}}{\mathrm{m}^3}$)
α	void fraction
λ	thermal conductivity ($\frac{\mathrm{W}}{\mathrm{m\,K}}$)
λ_{clad}	thermal conductivity of Genesis rod cladding ($\frac{\mathrm{W}}{\mathrm{m\,K}}$)
μ	dynamic viscosity (Pa s)
ν	kinematic viscosity ($\frac{\mathrm{m}^2}{\mathrm{s}}$)
σ	surface tension ($\frac{\mathrm{N}}{\mathrm{m}}$)
τ	time constants (s)
φ''_q	heat flux ($\frac{\mathrm{W}}{\mathrm{m}^2}$)
ϕ_e	total energy flow (W)
ρ	density ($\frac{\mathrm{kg}}{\mathrm{m}^2}$)

Dimensionless numbers:

$\mathrm{Pr} = \frac{\nu}{a}$	Prandtl number
$Nu = \frac{hD}{\lambda}$	Nusselt number
$Ra = v\sqrt{\frac{\rho D}{\sigma}}$	Rayleigh number

3. Theoretical background

3.1 Governing equations

For the conduction of heat in a cylindrical rod, an equation can be derived from the diffusion equation

$$\frac{\delta T}{\delta t} = a\nabla^2 T \ + q''' \tag{3.1}$$

In the one-dimensional case (to the radius r), the diffusion equation can be simplified to

$$\frac{\delta T}{\delta t} = \frac{1}{r}\frac{\delta}{\delta r}\left(r\frac{\delta T}{\delta r}\right) + q''' \tag{3.2}$$

Equation 3.2 governs all heat conduction and generation inside the rod. For the particular case a more or less uniformly distributed heat production in the $r-$direction inside the rod, a solution for the temperature can sometimes be found analytically, depending on the boundary conditions. For this see for example Van der Hagen (1988) [1]. However, in the forthcoming experiment a situation is examined for which an analytical expression for the transient temperature profile cannot easily be found. Instead, a number of simulations will be conducted to study the process of heat conduction in the rods for different situations.

The same equations can of course be applied to the heat transfer from the rod to non-convective surrounding media. In the case of a convective coolant, Newtons law of cooling can be used to describe the heat transfer process:

$$\varphi_q'' = h\Delta T \tag{3.3}$$

In which φ_q'' is the heat flux from the rod to the coolant, h is the heat transfer coefficient and ΔT represents the temperature difference between the rod surface and the surroundings. The main difficulty in the application of expression 3.3 is finding a correct expression for h. The dimensionless form of h is named the Nusselt number (Nu) [2]:

$$Nu = \frac{hD}{\lambda} \tag{3.4}$$

For the case of a horizontal rod in free convection, the following general relation for the mean Nusselt number is given by Churchill and Chu [3] and is valid over a large range of data:

$$\overline{Nu}_D^{1/2} = 0,60 + \frac{0,387 Ra_D^{1/6}}{\left[1 + (0,559/\,\mathrm{Pr})^{9/16}\right]^{8/27}} \tag{3.5}$$

for $10^{-5} \leqslant Ra_D \leqslant 10^{12}$, in which Ra_D and Pr are the Rayleigh number and the Prandtl number respectively. An exact correlation for the mean Nusselt number for a vertical setup of multiple rods and a saturated boiling Freon coolant, as is the case in the Genesis experiments is hard to find. A composite relation by Chen [4], which covers the entire range of saturated boiling, can be used here. The heat transfer rate can be expressed as

$$\varphi_q'' = h_{2\Phi}(T_w - T_{sat}) \tag{3.6}$$

given the bulk fluid temperature is at saturated conditions. The two phase heat transfer coefficient ($h_{2\Phi}$) can be divided into two parts; a term due to nucleate boiling (h_{NB}) and a term due to convection heat transfer(h_c):

$$h_{2\Phi} = h_{NB} + h_c \tag{3.7}$$

The nucleate boiling term can be described as follows:

$$h_{NB} = S(0,00122)\left[\frac{\left(\lambda^{0,79} c_p^{0,45} \rho^{0,49}\right)_f}{\sigma^{0,5} \mu_f^{0,29} h_{fg}^{0,24} \rho_g^{0,24}}\right] \Delta T_{sat}^{0,24} \Delta p^{0,75} \tag{3.8}$$

$$S = \frac{1}{1 + 2,53 \times 10^{-6}\,\mathrm{Re}^{1,17}} \tag{3.9}$$

Where subscript $_f$ indicates values for the properties of the coolant as a liquid and $_g$ for the coolant in gaseous form. The convective part is even more complex. It is a modified Dittus-Boelter correlation given by:

$$h_c = 0,023\left(\frac{G(1-x)D_e}{\mu_f}\right)^{0,8} (\mathrm{Pr})_f^{0,4} \frac{\lambda_f}{D_e} F \tag{3.10}$$

$$F = 1, \qquad \text{for } \frac{1}{X_{tt}} < 0,1 \tag{3.11}$$

$$F = 2,35\left(0,213 + \frac{1}{X_{tt}}\right)^{0,736} \qquad \text{for } \frac{1}{X_{tt}} > 0,1 \tag{3.12}$$

$$\frac{1}{X_{tt}} = \left(\frac{x}{1-x}\right)^{0,9} \left(\frac{\rho_f}{\rho_g}\right)^{0,5} \left(\frac{\mu_g}{\mu_f}\right)^{0,1} \tag{3.13}$$

3.2 Thermocouples

In this section, we will refrain from explaining the physical processes inside thermocouples that produce the measurable difference in electrical potential. For detailed information on this subject, see for example [5] or [6]. It will suffice to say that for a certain temperature gradient the distinct conductors of the thermocouple will produce a potential difference. This potential difference (U_{ab}) between wire a and b is dependent on a proportionality constant S and the temperature difference ΔT between the hot and the cold junctions:

$$U_{ab} = S\Delta T \tag{3.14}$$

Of course, the thermocouple used in the experiments has to be calibrated. A K-type thermocouple (Chromel/Alumel) is used and although reference tables are widely available (in the enclosed information by the manufacturer [7] and also for example at the instrumentation central site [8]) , it is important to know if these tables apply in the circumstances in which the experiment is conducted . The reference table seems to indicate that in the temperature range from 20 to 40 °C the potential difference is related linearly to the temperature of the thermocouple. This means we can easily find a conversion factor (a value for S) if it indeed turns out that the table applies to our thermocouple in our situation.

3.3 Transfer functions

3.3.1 Laplace Transformations

A transfer function (in this report indicated with a capital G and usually in subscript the system for which it is a transfer function) is a mapping of the Laplace transform of an input signal to an output signal [13]. It is mainly used in linear, time-invariant (LTI) systems. If x(t) is an input signal to a LTI system and y(t) is the output signal and their corresponding Laplace transforms:

$$\begin{aligned} X(s) &= \int_{-\infty}^{\infty} x(t)e^{-st}dt = \pounds\{x(t)\} \\ Y(s) &= \int_{-\infty}^{\infty} y(t)e^{-st}dt = \pounds\{y(t)\} \end{aligned} \tag{3.15}$$

Then the output is related to the input by the transfer function $G(s)$ as:

$$Y(s) = G(s)X(s) \tag{3.16}$$

So if the transfer function of a system is known, it is possible to determine the output signal for every input signal. When $Y(S)$ is transformed back

into the time domain with the inverse Laplace transform:

$$y(t) = \frac{1}{2\pi i} \int_{\sigma-i\infty}^{\sigma+i\infty} Y(s)e^{st}ds = \mathcal{L}^{-1}\{Y(s)\} \tag{3.17}$$

(with s split into a real and imaginary part $s = \sigma+i\omega$), we have an expression for the output signal. A number of different methods can be employed to find the transfer function for a certain system. In this experiment it is done by recording the response to a step function and subsequently calculating G with the help of equations 3.15 and 3.16. For instance, for a first order system

$$\tau\frac{dy(t)}{dt} + y(t) = x(t) \tag{3.18}$$

this derivation of G would proceed in the following manner. First the Laplace transforms can be calculated with the help of equations 3.15, or a Laplace transform table [16]. Equation 3.18 now becomes:

$$\tau sY(s) + Y(s) = X(s) \tag{3.19}$$

According to equation 3.16 the transfer function will now be:

$$G(s) = \frac{Y(s)}{X(s)} = \frac{1}{s\tau + 1} \tag{3.20}$$

As explained above, the input signal $x(t)$ will be a step function, which has the Laplace transform:

$$\begin{aligned} x(t) &= u(t) \\ X(s) &= \frac{1}{s} \end{aligned} \tag{3.21}$$

where $u(t)$ denotes the step function. The output signal can now be calculated:

$$Y(s) = G(s)X(s) = \frac{1}{s(s\tau + 1)} \xrightarrow{\mathcal{L}^{-1}} y(t) = (1 - e^{-\frac{t}{\tau}})u(t) \tag{3.22}$$

This means that at $t = 0$ (the moment the step function is applied as an input to the system) the response will show output $y(t) = (1 - e^{-\frac{t}{\tau}})$ also starting at $t = 0$. The output calculated above is thus the response of a first order system to a step in the input. Therefore if we see a similar response to a step in $x(t)$ in our experiment, we can be pretty sure the system involved is a first order system. For second or higher order systems similar derivations can be done to find the system transfer function.

Special attention should be given to the parameter τ. This parameter is called the *time constant* of the system. It is a measure for the rate at which

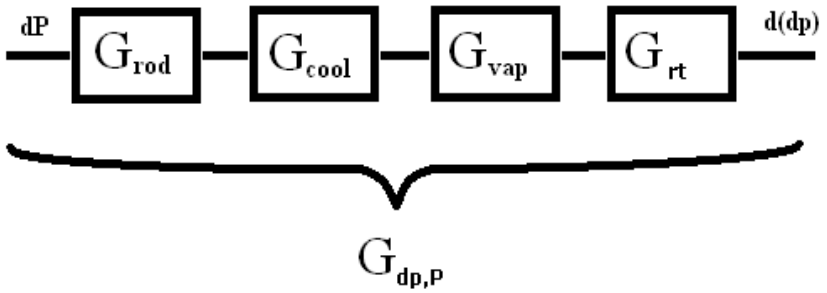

Figure 3.1: Total transfer function $G_{dp,P}$, consisting of four main contributions; the rod transfer function (G_{rod}), coolant transfer function (G_{cool}), vaporisation transfer function (G_{vap}) and the residence time transfer function (G_{rt})

the first order system responds. As τ decreases, the rise time of the step response becomes shorter and the other way around. The most important information about a system is therefore contained in the time constant. A first order system has only one time constant, but higher order systems usually have more that one.

Finally, if several different systems are combined, of which the separate transfer functions G_1, G_2, ..., G_n are known, the total transfer function is just a simple multiplication of the parts:

$$G_{total} = G_1 G_2 ... G_n \tag{3.23}$$

As stated in the introduction, one of the main reasons for conducting this experiment is finding out which factor is limiting to the rate of the heat transfer from the rod to the coolant. In figure 3.1 the total transfer function $G_{dp,P}$ for the measurements at the Genesis facility is schematically divided into parts that make up the main contributions to the total transfer function from a change in power (dP) to a change in pressure drop over the core ($d(dp)$). We are able to influence dP and we can measure $d(dp)$. Therefore in all Genesis measurements these four contributions will be present.

3.3.2 Sinusoidal signals

A special case of transfer functions occurs when the input signal is a sinusoid. As it is the sum of two complex exponentials, we can predict the output

voltage directly by examining the transfer function. The input $x(t)$ will be of the following form:

$$x(t) = A\sin(\omega t) \tag{3.24}$$

which can be written as the sum of two complex exponentials:

$$x(t) = \frac{A}{2i}\left(e^{i\omega t} - e^{-i\omega t}\right) \tag{3.25}$$

The output $y(t)$ for LTI systems will be of the same form as $x(t)$, with only one difference; the complex amplitude of each of the exponential terms in $x(t)$ is multiplied by the transfer function $G(\omega) = |G(\omega)|\, e^{i\arg(G(\omega))}$, evaluated at each exponential's frequency $\omega = 2\pi f$. It will look like this:

$$y(t) = \frac{A}{2i}\left(G(\omega)\cdot e^{i\omega t}\right) - \frac{A}{2i}\left(G(-\omega)\cdot e^{-i\omega t}\right) \tag{3.26}$$

Which, since $|G(\omega)| = |G(-\omega)|$ and $\arg(G(-\omega)) = -\arg(G(\omega))$, can be written as and finally simplified to:

$$\begin{aligned} y(t) &= \frac{A}{2i}\,|G(\omega)|\, e^{i(\omega t + \arg(G(\omega)))} - \frac{A}{2i}\,|G(\omega)|\, e^{-i(\omega t + \arg(G(\omega)))} && (3.27)\\ &= A\,|G(\omega)|\sin(\omega t + \arg(G(\omega))) && (3.28) \end{aligned}$$

So, using Johnson's words to put this simply [19], the circuit's output to a sinusoidal input is also a sinusoid, having a gain equal to the magnitude of the process transfer function and a phase shift equal to the argument of the transfer function at the source frequency.

4. The Genesis facility

The Genesis facility is an experimental setup at the physics of nuclear reactors group at the R3 department of Delft University of Technology. It is built to answer questions about the stability of a new reactor type by General Electric; the Economic Simplified Boiling Water Reactor (ESBWR). The Genesis setup is a scaled and simplified model of the ESBWR. It is schematically presented in figure 4.1.

Part of the scaling is the use of Freon (R134a) as a coolant instead of water. To guarantee a simple and low cost experimental setup that is easily accessible, electrically heated rods are used instead of Uranium rods. These rods are heated by a resistance wire in their centres, which are lined with Magnesium Oxide. Of course, these heating rods have a different heat transfer characteristic than the ESBWR uranium rods, while we do want them to respond similarly to changes in void fraction in the core. This problem can be solved by determining the transfer function of the Genesis rod alone, eliminating it from the Genesis facility cumulative transfer function (i.e. the response of the coolant temperature to a change in power input) and replacing it by a simulated Uranium rod characteristic. As stated in the introduction, one of the goals of this experiment is to determine the transfer function of a Genesis heating rod.

Many physical properties are continuously monitored throughout the Genesis facility and can be recorded by a computer by means of a National instruments DAQ/MX data input card. For our measurements, only a few of these are important. For instance, by recording the power dissipated in the core and the pressure drop over the core against time, we can determine the response of the latter to changes in the former. The more power is dissipated in the core the higher the temperature of the coolant will (eventually) get. Subsequently, the coolant will start boiling and create a change in the void fraction α in the core, which raises resistance to the flow through the core and thus creating an increase in pressure drop dp over the core. Also, it is the void created in this process that induces a natural circulation flow because of buoyancy forces. The connection between the power input and the pressure drop over the core is what we understand to be the 'Genesis facility total transfer function' $G_{dp,P}$ mentioned above. From this, and an expression for G_{rod} and G_{rt}(see figure 3.1), we could find G_{cool}; an expression for the heat transfer from the surface of a Genesis rod to the boundary layer of the surrounding coolant, regardless of the rod. That is, assuming that the

Figure 4.1: The Genesis facility schematically. Courtesy of reactor physics group, Delft University of Technology.

evaporation of the coolant happens so fast that it is of no importance (this means that G_{vap} in figure 3.1 will be assumed to be of no importance for the total transfer function, because the boiling process in the bulk is much faster than that of the heat transfer through the rod and boundary layer).

5. Experimental procedure

5.1 Strategy

The main goals of the experiment are to find the time constant(s) for the heat transfer through the Genesis heating rod and the time constants for the total heat transfer process in Genesis (i.e. the heat transfer from the resistance wire inside the rod to the coolant. Separately, this data will tell us how fast the heat transfer is and comparing them will give us information about which plays the most important role in the total heat transfer. Also, this information will tell us if the Genesis heating rods are an acceptable model for the uranium rods in the ESBWR.

To be able to find the time constants for the heat transfer and to determine what is the limiting and thus most important factor to the total heat transfer, we follow the approach below. In the remainder of the paragraph this strategy is clarified item by item in the chronological order of the experiment.

- First we conduct one dimensional numerical simulations for the heat transfer through only one Genesis heating rod. To be able to do a realistic simulation, we have to know exactly how the rod looks from the inside. Röntgen pictures of the Genesis rods are available from previous experiments.

- Secondly, we verify the numerical simulations by applying a power step to a Genesis rod outside the facility and comparing the measured temperature at the surface of the rod with the temperature predicted by the model. We opted for measurements (and thus simulations) in air.

- After verifying the model, we use it to determine the time constants for the heat transfer through one rod. This is achieved by imposing $T(t) = T(0)$ as boundary condition at the surface of the rod (this is similar to an infinitely fast transfer of heat to the bulk) and simulating the flux response to a step in the power input. From the obtained characteristic, the time constants can be found.

- Next, we determine the transfer function for the heat transfer in the Genesis facility by measuring the response of the pressure drop (dp)

over the core to changes in the input power (dP). As a lot of different processes play a role in Genesis, a sinusoidal power input is applied over a range of frequencies and from the gain and phase shift in dp, the time constants for the total heat transfer can be determined.

- Finally, as all the required time constants have been found, we can compare them and draw our conclusions.

5.2 Heat transfer simulation with Fortran 95

The heat transfer through the rod is complicated to such an extent that it is virtually impossible to find an adequate analytical solution for the heat transfer. For our purposes it is much more convenient to conduct a computer simulation of the heat transfer through the rod and from the rod to its surroundings. Naturally, the simulation needs to be verified with the aid of several measurements. If it turns out the simulation is an accurate representation of reality, we can use it for multiple purposes. For example, we can use it to determine the heat transfer characteristic for the heating rod alone, i.e. without taking into account its surroundings. This can be done by simply imposing the condition that the temperature be always the starting temperature at the edge ($T(t) = T(0)$), thus eliminating the second of the unknown transfer function squares in figure 3.1.

Also, when we impose the condition of a saturated boiling coolant, flowing vertically along the rod, we can determine if it is the heat transfer through the rod or the heat transfer to the coolant that is the limiting factor for the total heat transfer by comparing the new simulated heat transfer characteristic to the previous situation. This is one of the questions of interest.

The simulations will be done using a Fortran 95 compiler. The main algorithm for the heat transfer through the rod has been set up by M. Rohde [15]. As the rod is cylindrical and the deviation from a uniform heat dissipation profile can be easily calculated (equation 5.6), we can make do with a one dimensional numerical simulation. Therefore we only use one measure of extension: Δr. It signifies the length of one of the (very small) steps in the $r-$direction in which the $r-$domain is divided.

First, of course, equations 3.2 and 3.3 are converted to their numerical counterparts using an explicit numerical scheme, described in, among others,

Patankar (1980) [14]. Respectively they will be:

$$\begin{aligned} T(i,t+1) &= \Delta t \left(\frac{a}{(idr)\frac{dT}{dr}(i)} + a\frac{d^2T}{dt^2}(i) + \frac{q}{\rho c_p} \right) + T(i,t) \qquad (5.1) \\ \text{where:} \quad & \frac{dT}{dr}(i) = \frac{T(i+1,t) - T(i-1,t)}{2\Delta r} \\ \text{and} \quad : \quad & \frac{d^2T}{dr^2}(i) = \frac{T(i+1,t) - 2T(i,t) + T(i-1,t)}{\Delta r^2} \end{aligned}$$

for the diffusion equation, in which Δt and Δr are the time step and the length of one step in radius. i is an indicator for r. At the transition point between the MgO and the stainless steel of the cladding, we need to make a correction to this algorithm. The following condition must remain valid at this location:

$$\lambda_{MgO} \left(\frac{dT}{dr} \right)_{MgO} = \lambda_{cladding} \left(\frac{dT}{dr} \right)_{cladding} \qquad (5.2)$$

The numerical equivalent for this condition becomes:

$$T(i_{trans}, t+1) = \frac{\frac{\lambda_{MgO}}{\lambda_{cladding}}(T(i_{trans}-2,t) - 4T(i_{trans}-1,t)) - 4T(i_{trans}+1,t) + T(i_{trans}+2,t)}{-3 - 3\left(\frac{\lambda_{MgO}}{\lambda_{cladding}}\right)} \qquad (5.3)$$

and we impose this condition every timestep.

Newton's law can be numerically described as follows:

$$\frac{dT}{dr}(i = rod\ surface) = -\frac{h_{cool}}{\lambda_{clad}} T(i,t) \qquad (5.4)$$

Since it will solely be applied as a boundary condition on equation 5.1 for calculations at the rod surface. In equation 5.4 h_{cool} is the heat transfer coefficient from the rod surface to the coolant and λ_{clad} is the thermal conductivity of the rod cladding.

The explicit method that was used for the transition to the numerical model, is subject to one condition for the model to remain stable:

$$\Delta t < \frac{\rho c_p \Delta x^2}{2a} \qquad (5.5)$$

The material properties of the materials of which the rod is made (see figure 5.1) and the material properties of the surroundings, that are very important for an accurate numerical simulation, can be found in the Transport Phenomena Data Companion [16] and Binas [21]. The data material properties of Freon 134a is collected from separate sources, of which an extensive description can be found in bibliography entries [17] and [18]. To

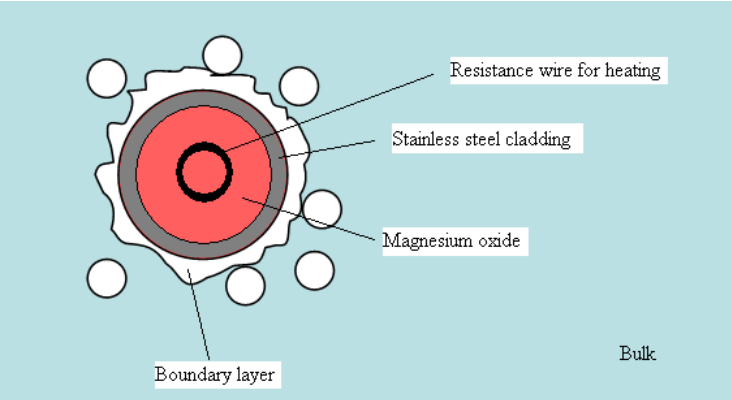

Figure 5.1: Cross-section of a Genesis heating rod, the cladding, resistance wire, boundary layer and filling are indicated. Picture (modified) courtesy of Martin Rohde, reactor physics department TUDelft.

make the simulation somewhat easier, we equate the material properties of the resistance wire to the properties of the Magnesium oxide. We do not expect this to lead to any problems, because the resistance wire is quite thin and the material properties of the Wolfram, of which the resistance wire is made, and the Magnesium oxide do not differ much.

5.3 Rod Geometry

To be able to make any claims about heat transfer within such an electrically heated rod, it is important to know how its interior looks like. It is known that the rod is heated by a resistance wire and filled with Magnesium oxide. This is held together by a cladding made out of stainless steel. In figure 5.1 the situation known thus far is shown in cross-section.

The exact measures in this cross-section are already known by previous Röntgen research within the department. Nevertheless, it is not well known how tight the resistance wire is wound. It is necessary to find out if the winding density varies, for that would disrupt the uniform axial heating profile of the rod. This can be done by taking new and very bright Röntgen pictures that make the distinct windings visible. Since the power that is dissipated per length unit varies linearly with the winding density, the power dissipated at a certain height can be calculated readily. So:

$$P \sim \Delta W \tag{5.6}$$

Where ΔW is the number of windings per unit length and P the dissipated power.

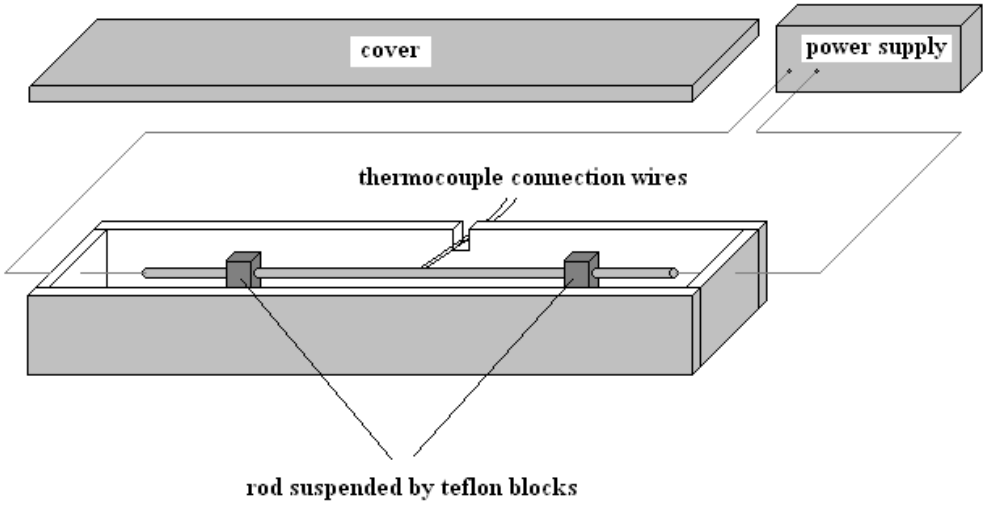

Figure 5.2: The experimental setup for temperature measurements on the surface of the rod.

5.4 Measurements at a single rod in free convection

5.4.1 experimental setup

To test our numerical model several measurements have to be done. In this case the choice is made to measure the temperature at the surface of one of the Genesis heating rods in air. The rod will be suspended horizontally in a sheltered environment to protect it from convective influences from the outside. The experimental setup is presented schematically in figure 5.2. The acquired temperature measurements will be compared to the predictions made by the simulated model. To be able to make accurate measurements we first have to make sure there will be no systematical errors in the equipment. In the next paragraphs it is made clear how this is achieved.

5.4.2 Amplification

Since the potential difference over the thermocouple junctions is in the order of microvolts per degree Celsius and the temperature range in which we are interested is approximately between room temperature and 40 °C, we need some form of amplification to measure a potential difference at all. We would like to work at an amplification factor of 1024 times. Of course we need to make sure that the amplifier will be able to amplify and transmit

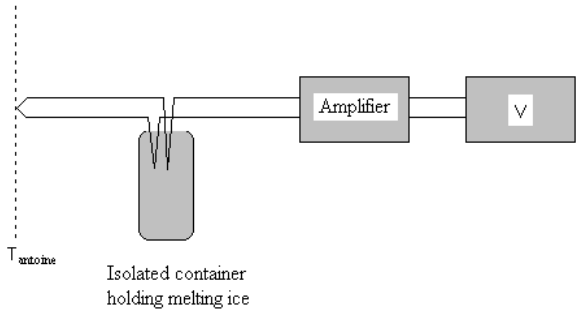

Figure 5.3: Thermocouple calibration setup. Reference junction is held at 0 °C.

fast changes in potential difference over the thermocouple, without attenuation at this amplification factor. Therefore we will determine the amplifier characteristic. That can be done by generating a fast oscillating signal with the Agilent function generator. By using an oscilloscope to visualize the input and the amplified signal, we can determine the amplification factor for different oscillation frequencies. Information about the equipment can be found in Appendix 2.

5.4.3 Thermocouple dynamics

A K type thermocouple (Chromel/Alumel) was used for all non-Genesis measurements. The thermocouple wires are insulated by a Teflon coating. More information about the thermocouple is enclosed in Appendix 2.

Thermocouple calibration

The easiest way of calibrating the thermocouple is by measuring the potential difference at the boiling point of water. The setup in figure 5.3 will be used to do this.The reference junction will be put into melting ice. However, this boiling point depends on the atmospheric pressure. Relations between pressure and the boiling point of water can be found in, for example, Thomsen [12]. The relation is given by Antoine's relation, an empirical relation for water:

$$\ln p_v = 16,573 - \frac{3988,842}{(T - 39,47)} \tag{5.7}$$

In which p_v is the vaporization pressure of water and T is measured in Kelvin. This can also be written as follows:

$$T_{antoine} = \frac{3988,842}{16.573 - \ln(P_v)} + 39,47 \tag{5.8}$$

In which $T_{antoine}$ is then the Temperature (in Kelvin) of boiling water according to Antoine's relation. Uncertainty equations for relation 5.8 can be found in Appendix 1. We can calculate $T_{antoine}$ for experiment conditions and compare it to the measured value (making use of the K type thermocouple tables composed by Instrumentation Central [8]). If these values do not contradict, we will use the given table, which is practically linear in the range of interest to us (20 to 40 °C), so we will be able to use the average value of $40,7\ \frac{\mu V}{°C}$. If it turns out the measured value is contradictory to the literature value, we will have to make some corrections to the table and use a second or third order polynomial to find new table values for our specific thermocouple. The criterion is thus formulated:

$$|T_{antoine} - T_{measured}| \leq\ 2\sqrt{(u(T_{antoine}))^2 + (u(T_{measured}))^2} \tag{5.9}$$

If condition 5.9 is met, the calculated and measured value are not contradictory.

Thermocouple transfer function

Even for a very small hot junction and very thin connection wires, the thermocouple itself will also take some finite time to start transmitting a change in potential difference (the junction first has to warm up or cool down itself). Therefore it is good practice to determine the heat transfer characteristic of the thermocouple itself. From this we will be able to see if the thermocouple is 'fast enough', i.e. to be of no significance in our measurements. This characteristic is found very easily. We leave the thermocouple at room temperature for a large period of time. Then, at $t = 0$ we will put it into a large container of hot (nearly boiling) water. We record the (amplified) potential difference characteristic with one of the Genesis data input cards. After repeating this measurement several times, we expect to be able to compare the heat transfer characteristic with a first order system, since the junction is made of metal and is only very small. That way we can consider it as a small sphere with uniform temperature. The energy balance

$$\frac{dE}{dt} = \phi_{e,in} - \phi_{e,out} + Production \tag{5.10}$$

for this situation (there is no net $\phi_{e,out}$ and it is clear there is no energy production inside the junction) now becomes:

$$\rho c_p V \frac{dT}{dt} = \phi_{e,in} \tag{5.11}$$

This is a first order system under the condition the heat transfer coefficient remains constant. As this is not completely true, we expect a step response from the thermocouple that resembles a first order system. When

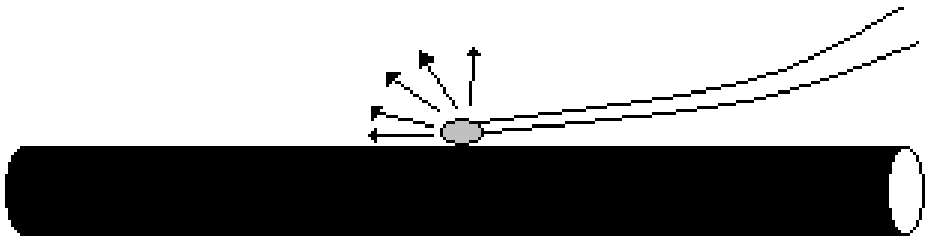

Figure 5.4: The thermocouple is spot welded to the rod.

we find its heat transfer characteristic (a solution to 5.11), we can determine how 'fast' the thermocouple is, in comparison to the heat transfer from rod to coolant.

Problems caused by thermocouple attachment method

Another transfer function arises when we consider the way we record the temperature on the rod surface. We cannot afford to break a rod for this experiment, so it is not possible to embed the thermocouple junction inside the cladding. Instead, the thermocouple will be attached to the rod by means of a spot weld, as shown in figure 5.4.

This method has a big disadvantage: The contact area between the hot thermocouple junction and the cladding is very small, especially in comparison to the contact area with the surrounding medium, so that it is bound to dissipate a significant amount of heat into the surrounding environment. This means that there will be an extra transfer function. To obtain a characteristic for this heat transfer, a number of measurements is done in which the thermocouple junction is suddenly brought into contact with a hot metal surface, using conducting paste to ensure a good connection between the metal surface and the thermocouple junction. For this situation, the same reasoning as in the previous paragraph is valid. Equation 5.11 will be only slightly different in this case:

$$\rho c_p V \frac{dT}{dt} = \left(\phi_{e,in} - \phi_{e,out}\right) \tag{5.12}$$

5.4.4 The total transfer function

The total transfer function for the setup shown in figure 5.2 consists of many different contributions and will look something like:

$$G_t = G_{\mathrm{sup}\,ply} \cdot G_{rod} \cdot G_{therm} \cdot G_{attachment} \cdot G_{amplifier} \cdot G_{ic} \cdot G_{computer} \cdot G_{rest} \tag{5.13}$$

Where $G_{\text{sup}\,ply}$ is the transfer characteristic of the power supply, G_{therm} and $G_{attachment}$ are, respectively, the transfer function related to the thermocouple itself and the attachment method, both described in section 5.4.3, G_{ic} the data input card transfer function, $G_{computer}$ the transfer function that relates the computer process input (=input card output) to the computer process output and finally the total transfer function for all other processes connected in the experiment, G_{rest}. To be able to say anything useful about G_{rod}, we have to either know the other transfer functions, or designate them not significant for our purposes (that means they are very close to 1 and can be neglected).

5.5 Measurements at the Genesis facility

Eventually, when the rod transfer function is found, we are interested in G_{cool}, the transfer function from the rod surface to the coolant in the Genesis facility. It can be extracted from the total transfer function $G_{dp,P}$, shown in equation 5.14.

$$G_{dp,P} = G_{rod} \cdot G_{cool} \cdot G_{vap} \cdot G_{rt} \tag{5.14}$$

Since the heat transfer process in the Genesis setup cannot be easily captured in a one-dimensional simulation, we will conduct measurements to find values for the time constants related to $G_{dp,P}$.

We will measure the response to a sinusoidal function and to a step function in the applied power. This can be done by measuring the pressure drop over the core while applying such a step or periodical function to it. When the coolant temperature rises, more vapor and thus more void will be created. This will increase resistance for the flow through the core. The result is an increase in pressure drop over the core. It must be remembered though, that there are two transfer functions concerned with this process, namely G_{vap} for the vaporization process and G_{rt} for the vapor residence time in the core. In using this method, we are assuming that the time it takes for Freon, heated to its boiling point, to turn into vapor is very short (at least much shorter than the time necessary for the heat transfer from the resistance wire to the Freon). This means, in fact, that we are neglecting G_{vap} shown in figure 3.1.

To guarantee as few feedback inside the reactor as possible (disturbances can make a full loop while the response is still being measured), a pump is used to generate a forced flow over the core that remains (approximately) constant, although the natural circulation effect is still present an has some influence on the flow. Unfortunately the pump causes a lot of extra noise on the measurements, which can only be partially filtered away. This makes it necessary to do periodical measurements with a lot of recorded periods per frequency, so the precision of the calculated time constants will increase.

By comparing the input and the output signals for sinusoidal signals at different frequencies, we can find the gain and the phase shift, which means by equations 3.25 and 3.28 that we can find the transfer function for the total system.

6. Results and Discussion

6.1 Determining the rod geometry and local winding density

From previous research in the Physics of Nuclear Reactors group, a number of Röntgen pictures is available to study the inside of the heating rods. Especially the thickness of the cladding, the diameter of the winding of the resistance wire is important. These measures, along with the length and diameter of the rod can be found in table 6.1.

This information alone is not enough to guarantee that the simulation is in accordance with measurements anywhere on the rod surface. For example the location and winding density of the resistance wire could vary and that could influence the local power dissipation. Therefore we need to determine on what (vertical) location of the rod we will conduct the temperature measurements for the verification of the model and take a detailed Röntgen picture of this location.

A number of new and very bright Röntgen pictures were taken of a rod with the thermocouple, for later temperature measurements, already welded to it. This makes it possible to determine the winding density at the exact location of the thermocouple, as can be seen in figure 6.1. It turns out that the windings are closer to each other at this location than on average over the rod, which means that more power is dissipated locally (than on average). The local winding density at the thermocouple location is $8.55\,\mathrm{cm}^{-1}$ $\left(\pm 0,05\,\mathrm{cm}^{-1}\right)$ against an average winding density over the whole rod of $8,0\,\mathrm{cm}^{-1}$ $(\pm 0,05\,\mathrm{cm}^{-1})$, which comes down to a $6,88$ % increase. Equation 5.6 tells us that the connection is linear, which means the power

Table 6.1: Important measures of a Genesis rod

Rod diameter	6,16 mm
Rod length	1,41 m
Resistance wire winding diameter	2,78 mm
diameter of MgO (including resistance wire)	5,26 mm
Thickness of the cladding	0,45 mm
thickness of resistance wire	0,3 mm

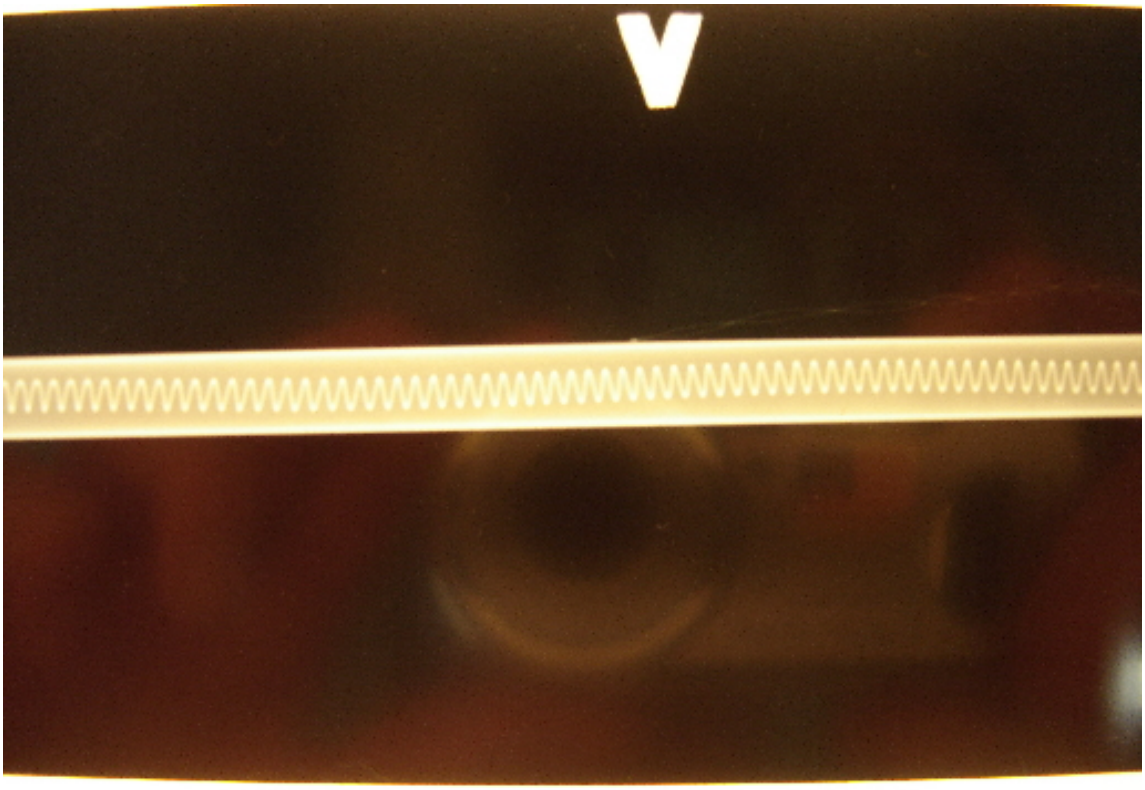

Figure 6.1: Röntgenpicture of Genesis heating rod. The resistance wire, the cladding and even the thermocouple junction (small dot indicated by the arrow), can be seen. In the original, the thermocouple wires can also be seen clearly.

is locally increased by the same factor. This means that to match future measurement data at this location, a simulation can be performed with a power increase of $6,88$ %. Considering the simulation being one-dimensional, this can be done without problems. For verification purposes the simulations will therefore be conducted at 171 W power input, while the measurements are done at 160 W.

In figure 6.1 it can also be noticed that the resistance wire does not remain straight in the center of the heating rod. However, as it is very nearly straight and centered at the thermocouple location, we have chosen to neglect this effect.

6.2 Thermocouple calibration

The air pressure during the model verification measurements was $1,0151$ bar with an uncertainty of $0,0005$ bar. According to the literature [20], the uncertainty in Antoine's relation is maximally $26,6 \cdot 10^{-5}$ bar. With the help of equation 5.7, the boiling point of water is found to be $100,03\,^{\circ}\mathrm{C}$ with a corresponding uncertainty (by equation A.1 and A.2) of $0,13\,^{\circ}\mathrm{C}$. The average potential difference (over a period of 15 s) over the thermocouple in boiling water, measured with the reference setup in figure 5.3, is $4,095$ mV plus or minus the last digit on the multimeter. By linear interpolation this relates to $100,0\,^{\circ}\mathrm{C}$ according to the thermocouple reference table [5], with an uncertainty of $0,10\,^{\circ}\mathrm{C}$ because of the uncertainty of the voltage registration of the last digits in the computer. By applying relation 5.9 it becomes clear that these two values are not contradictory and the thermocouple functions well in our experimental surroundings. There is no need to create a new, adjusted reference table. This also means, since the table indicates that in the temperature range between $20\,^{\circ}\mathrm{C}$ and $40\,^{\circ}\mathrm{C}$ the potential difference and the corresponding temperature relate practically in a linear manner, that we can use the value of $0,0407\,\frac{\mathrm{mV}}{^{\circ}\mathrm{C}}$ to translate the measured potential differences to temperatures.

6.3 Thermocouple dynamics

6.3.1 Thermocouple transfer function

With the method described in the section 5.4.3, a characteristic for the response to a sudden change in temperature is obtained for the thermocouple. This characteristic is shown in figure 6.2. Our expectation was (equation 5.11) that the response of the thermocouple would come very close to a first order response. Judging by figure 6.2 this indeed seems to be the case. The time constant for the (first order) thermocouple transfer function G_{therm} is determined to be 11 ms with an uncertainty of $0,5$ ms by fitting it in Origin.

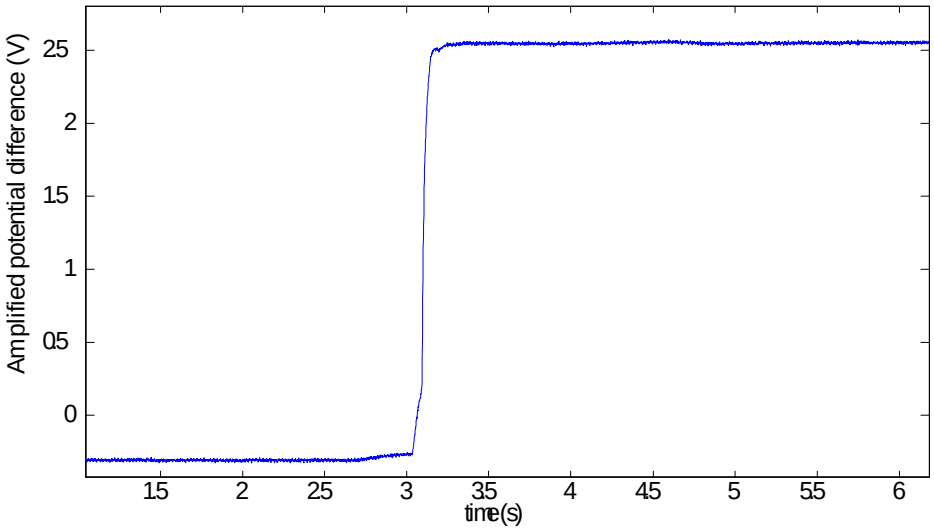

Figure 6.2: Thermocouple response to submerging it in hot water at a certain moment in time t.

Since the time constants for the heat transfer through the rod and for the coolant are expected to be much larger (at least in the order of tenths of seconds), this transfer function can be deemed unimportant for our purposes and can therefore be neglected, so $G_{therm} \approx 1$.

6.3.2 Thermocouple attachment transfer function

The transfer function for the measurement method turns out to be a significant factor for the temperature measurement. In figure 6.3 the total response is shown. It can be seen that the potential difference already starts to increase before the thermocouple junction reaches the hot wall at $t \approx 550\,\text{ms}$ in figure 6.3. This is due to the fact that the thermocouple is already slightly heated by radiation coming from the wall, before it actually touches it. In spite of this effect the response is still taken to be of the first order. Therefore the first part of the recorded response is cut off to let the moment the thermocouple touches the hot wall coincide with $t = 0$. In figure 6.4 the (filtered) response to a sudden contact to a heated surface is shown and compared to the best first order system fit. As expected, the response approaches the first order system very closely. From figure 6.4, it can also be seen that the response can be encapsulated in the following equation:

$$y(t) = -1,5e^{(-\frac{t}{0,369})} + 2,129 \tag{6.1}$$

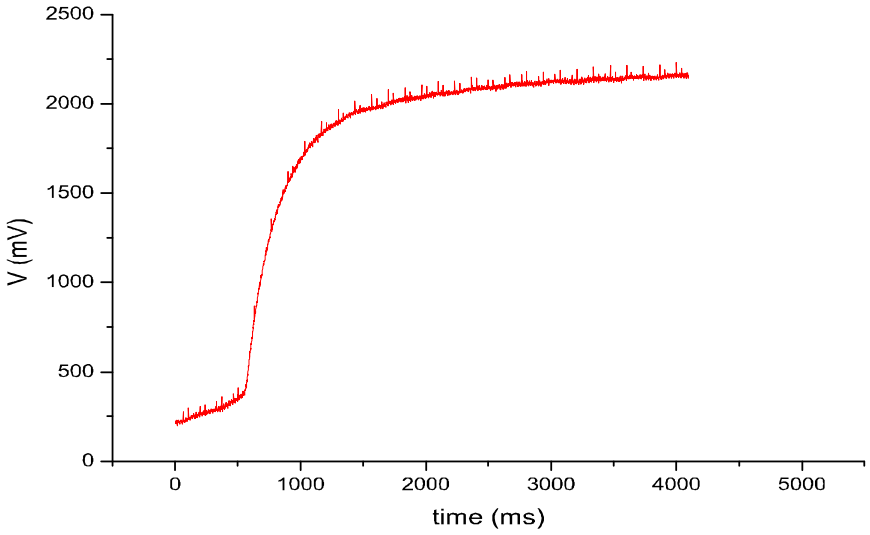

Figure 6.3: Measurement method response to sudden contact to metal surface.

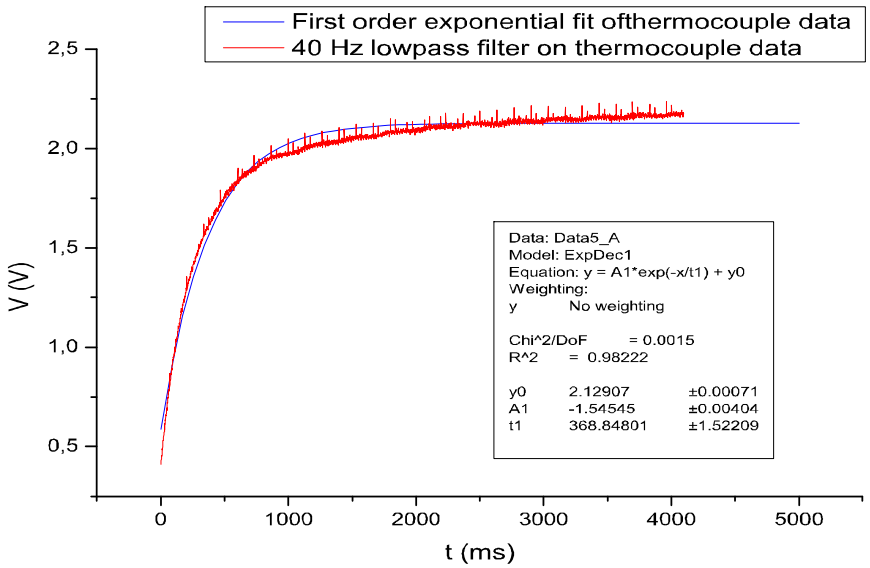

Figure 6.4: Measurement method response to sudden contact with heated metal surface, compared to the best fitting first order system.

Although this is not a very 'clean' (i.e. at $t = 0$, $y(0) \neq 0$) fit, the only information we need from equation 6.1 is the time constant. If we fill in this parameter for a standard first order system, we will get a normalized response to a step function.

$$G_{attachment} = 1 - e^{-\frac{t}{0,37}} \tag{6.2}$$

With a time constant of almost $0,37$ s, the transfer function will influence our temperature measurements and has to be taken into account in the verification of the simulations.

One remark remains; What effect causes the small peaks in the graph that seem to appear periodically? After an extensive search for possible noise in the equipment and the measurement method used, the most probable explanation is that the peaks show the experimenter's heartbeat. The thermocouple was held by hand while conducting the experiments and it must be remembered the amplification factor is 1024 times. The same potential differences that are measured while recording a cardiogram where apparently picked up by the thermocouple and wound up in the measurements. Fortunately, the peaks do not seem to cause any major problems in determining the characteristic.

6.4 Amplification

In section 3.4.1 it was made clear that we need some form of amplification for the thermocouple output signal. However, when the input signal reaches a certain frequency, the amplification factor drops. We call this frequency the cut-off frequency. By using an oscilloscope and a function generator, the cut-off frequencies can be determined. In table 6.2 the results are shown, as well as the real (measured) amplification factors. Because of the noise, the uncertainty in the higher amplification factors is quite large, as can also be seen in table 6.2.

This shows that frequencies well above 1kHz, the frequency at which we are planning to acquire data with the computer data input card, are recorded without attenuation. So we can conclude that $G_{amplifier} \approx 1$.

6.5 Other transfer functions

It is clear from the overview equation 5.13, that many more transfer functions are to be determined to be able to say anything about G_{cool}. Luckily, the transfer functions of all Genesis equipment has already been determined from previous measurements [23]. The time constant for the total transfer from computer signal to supply and from data acquisition card back to the computer has been calculated to be 4 ms. This is such a small value that

Table 6.2: Measured amplification factors at 1 kHz compared to the indicated amplification factors, as well as the cut-off frequencies at every amplification factor

indicated ampl. factor	measured ampl. factor	Cut-off frequency (kHz)
1	$1,0 \pm 0,2$	$15,0 \pm 0,2$
2	$2,0 \pm 0,2$	$14,9 \pm 0,2$
4	$4,0 \pm 0,2$	$15,0 \pm 0,2$
8	$8,0 \pm 0,5$	$15,2 \pm 0,2$
16	$16,0 \pm 0,5$	$15,4 \pm 0,5$
32	$32,0 \pm 2,0$	$15,0 \pm 0,5$
64	$64,0 \pm 3,0$	$15,0 \pm 0,5$
128	$132 \pm 5,0$	$14,9 \pm 0,5$
256	$250 \pm 5,0$	$14,9 \pm 0,5$
512	528 ± 20	$5,0 \pm 0,5$
1024	1056 ± 80	$3,5 \pm 1,0$

we have decided to neglect these transfer functions, considering the time constants of the heat transfer processes are expected to be in the order of seconds. So one could say we have put $G_{\mathrm{sup}\,ply} \cdot G_{ic} \cdot G_{computer} \cdot G_{rest} = 1$.

6.6 Heat transfer simulation for a single rod

With the help of equations 5.1 and 5.4, a one-dimensional algorithm could be written that simulates heat transfer through the rod and from the rod to its surroundings. For different situations only the boundary conditions are adjusted. The algorithm for a single Genesis rod in air is included in Appendix 3.

In figure 6.5 the simulated flux development at the rod surface is shown, imposing the boundary condition $T_{surface}(t) = T_{surface}(0)$. As a result we obtain a flux characteristic of the rod only. Some observations can already be done concerning verification of the model. First of all, it is clear that when the heat transfer becomes a steady state process, the outgoing heat flux should match the production of heat inside the rod. As the heat production per unit length was set at 160 W while creating figure 6.5, the heat flux at the surface should be $\frac{160}{A_{rod}} = 5874 \frac{\mathrm{W}}{\mathrm{m}^2}$. The curve in figure 6.5 approaches that value very well. Secondly, we notice that the characteristic resembles a (overdamped) second or higher order response to a step function. If the simulations can be verified by measurements, we could fit a second or third order response to figure 6.5 and find its time constants with the aid of equations 3.15 and 3.16.

Nevertheless, to verify the model with reality, we selected the case of a

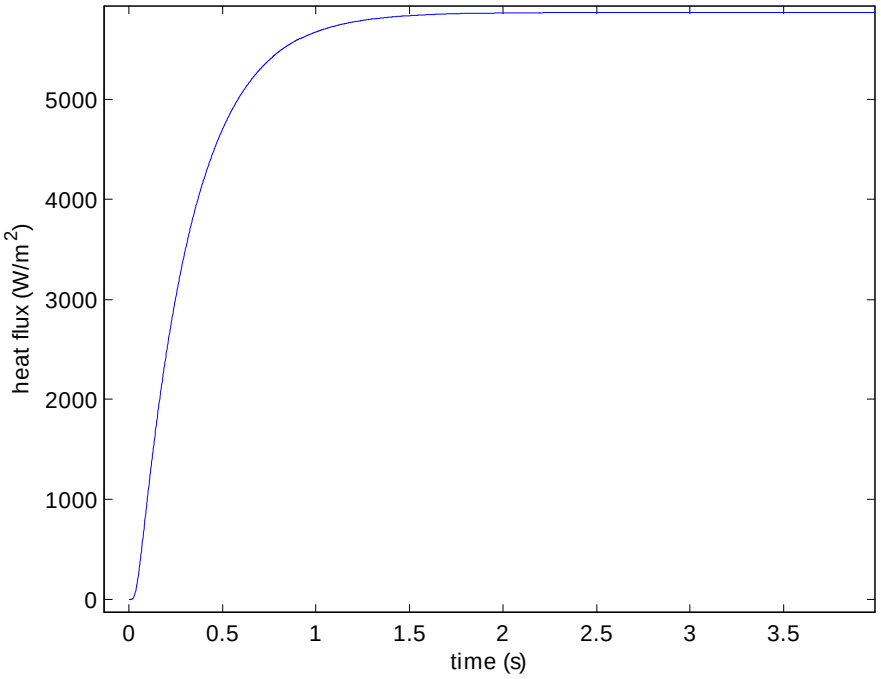

Figure 6.5: Simulated flux development at the rod surface for $T_{surface}(t) = T_{surface}(0)$.

horizontal rod in free convection in air, since we cannot perform temperature measurements at the surface of the rod and keep the surface temperature at $T_{surface}(0)$ at the same time. The surface temperature against time, calculated by the model, can be found in figure 6.6. Since we are mainly interested in the first few seconds of the response (since that is in the order of magnitude we expect the time constants to be), only these are shown in the figure.

6.7 Verification of the numerical model

Now that we know that the thermocouple is suited for our purposes and the amplifier won't cause any attenuation problems, we can compare the simulation results to the measurements done on the horizontally suspended rod in air in free convection. It is only possible to compare the first part of the responses, since there are some practical problems concerning measuring at higher temperatures (the protective environment edge is reached and the full free convective system breaks down or the rod could get too hot, since it is cooled insufficiently in air). In figure 6.7 the two are compared (the measurements at 160W and the simulation at 171W as described above). On first view the simulation seems to coincide with the measurement data reasonably well. However, at a second glance it turns out that although the temperature increases at the same rate eventually, in the first one or two seconds, the two graphs are quite different. In reality it seems to take longer for the temperature at the surface to start rising. In other words, the measurement seems to be 'slower' than the simulation. Yet, we do have a possible cause for this discrepancy, being the dynamics of the surface welded thermocouple (recall figure 6.4).

As there is quite some noise incorporated in the measurement signal, it is impossible to simply eliminate this transfer function by means of Laplace transformations (equations 3.15 and 3.16), without increasing uncertainty in the signal drastically. However, it is possible to 'add' the transfer function to the simulated signal without too much trouble with the help of the same equations. This is done by taking the Laplace transform of both the simulation and the thermocouple measurement method response (equation 6.1), multiplying these two and inverse Laplace transforming the result. The transformations are conducted in Matlab. In figure 6.8this result is shown. It can be seen in this figure that the measurement data now matches the simulation quite well, including the first two seconds. Indeed it matches the simulation data so well that we can conclude that the simulations are verified sufficiently. Also, the fact that the heat flux reaches the correct value when the heat transfer becomes steady state (as is shown in section 6.2) , encourages us to rest assured the numerical model and the simulations are correct.

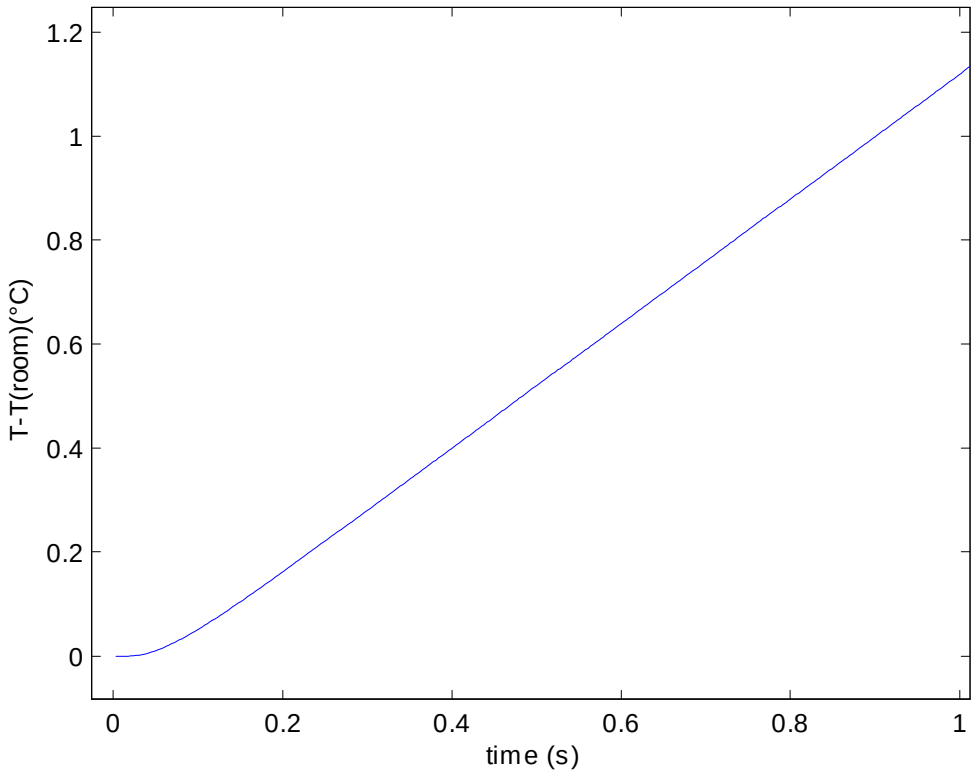

Figure 6.6: Simulated heat transfer of horizontal rod in air in free convection.

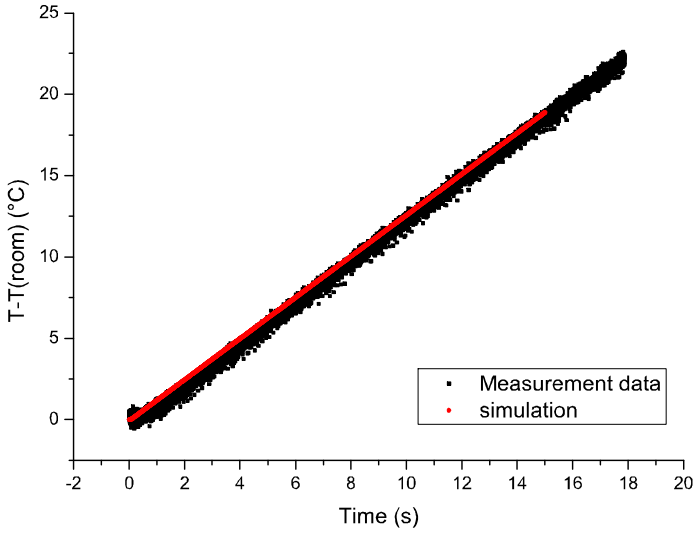

Figure 6.7: Temperature measurement compared to the temperature predicted by the numerical simulation of a horizontally suspended rod in air.

6.8 Transfer Functions and time constants

6.8.1 Heating rod

Now that we have demonstrated that the simulations are in accordance with reality, figure 6.5 can be fitted in Origin to find the time constants. We have already noticed that the curve has the properties of a (overdamped) second or higher order system response to a step function. It is therefore fitted with a second order system response that looks like this:

$$y(t) = A_1 e^{-\frac{t}{\tau_1}} + A_2 e^{-\frac{t}{\tau 2}} + y_0 \tag{6.3}$$

The time constants τ_1 and τ_2 are found to be $0,030\,\mathrm{s}$ and $0,28\,\mathrm{s}$ respectively after a large number of least square fitting iterations in Origin. System fitting information can be found in figure E in Appendix 5.

6.8.2 Simulating a vertically suspended heating rod in Freon 134a

By means of equations 3.6 to 3.13, we can find an expression for the mean heat transfer coefficient over the height a Genesis rod, for a vertically positioned rod in (saturated) boiling Freon. This is done for the experimental

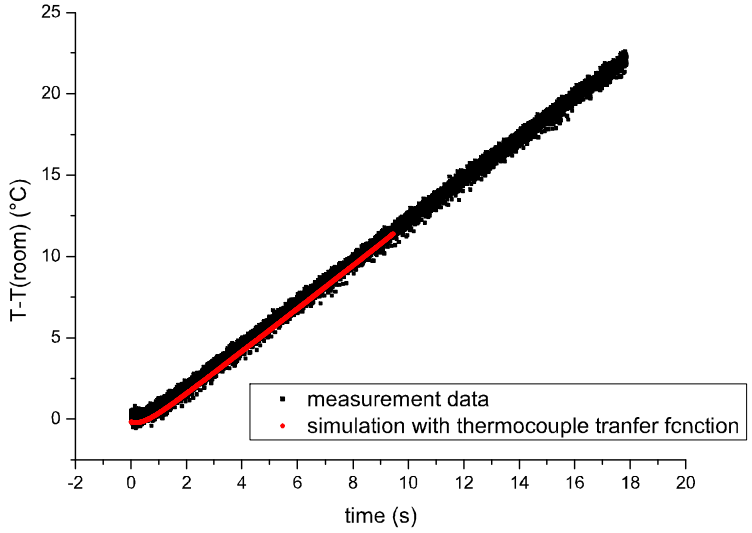

Figure 6.8: Temperature measurement at rod surface, compared to simulated temperature in which a thermocouple attachment transfer function is artificially included.

conditions as encountered in the Genesis setup, at nominal conditions (25 kW dissipated in the core) with a forced flow of $1700 \frac{\text{kg}}{\text{m}^2\,\text{s}}$. The expression for $h_{2\Phi}$ still depends on the temperature and pressure and has to be incorporated as a boundary condition in the algorithm. The rest of the data used to calculate the relation for $h_{2\Phi}$ can be found in Appendix 6 and the relation between the void fraction and the quality, which is based on the HEM approximation [3], is given as follows:

$$\{\alpha\} = \frac{1}{1 + \frac{1-x}{x}\left(\frac{\rho_g}{\rho_f}\right)} \tag{6.4}$$

Now, a response for this particular system can be simulated. The simulated temperature at the surface of the rod against time, is shown in figure 6.9. After comparing the response in Freon with the second order system in equation 6.3, we find that $\tau_1 = 0.12\,\text{s}$ and $\tau_2 = 0.75\,\text{s}$ after a large number of least square fitting iterations. Fitting information can be found in Appendix 5 (figure E.1).

6.8.3 Genesis response to a power step

Now that we have a simulated step response for a vertically suspended rod in the Genesis conditions, the most simple way to conduct a quick reality check, is by imposing a step function to the Genesis power input and record the response. For this purpose we record the pressure drop over the core, because it is (as explained in the last section of Chapter 4) a good measure for the temperature of the coolant. We expect the simulated step response to rise faster, since we have not incorporated the vapor residence time transfer function G_{rt} in the simulation yet. To be able to compare both responses, the temperature simulation is normalized at the maximum value of the Genesis step response. The Genesis response to a 4000 W power step is shown in figure 6.10, as is the simulated temperature response.

We notice that the simulation indeed rises faster, as was expected, but it is so much faster (a first order model with a time constant τ of $3,5$ s seems to be a better approximation), that we can conclude that G_{rt} is either very slow or there is some other unknown effect that introduces an new transfer function. It is clear that the noise in figure 6.10 is very dominant. To find out more about G_{rt} and a possible unknown additional transfer function G_{add}, we will conduct measurements with an oscillatory power input signal.

6.8.4 Genesis heat transfer for oscillatory conditions

In the last section of the previous chapter we have already explained that the best way to find the time constants, due to high noise ratios from the pump, is applying a sinusoidal signal for a range of frequencies and compare the output to the input signal in terms of gain and phase shift. Analyzing

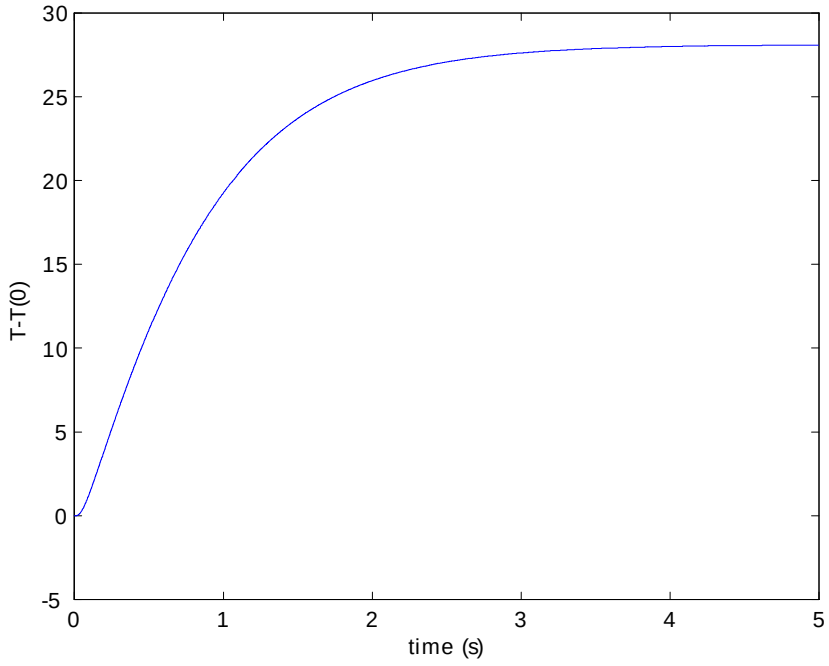

Figure 6.9: The simulated response to a sudden step in power of the rod without taking its surroundings into account and the simulated response of the rod in freon 134a.

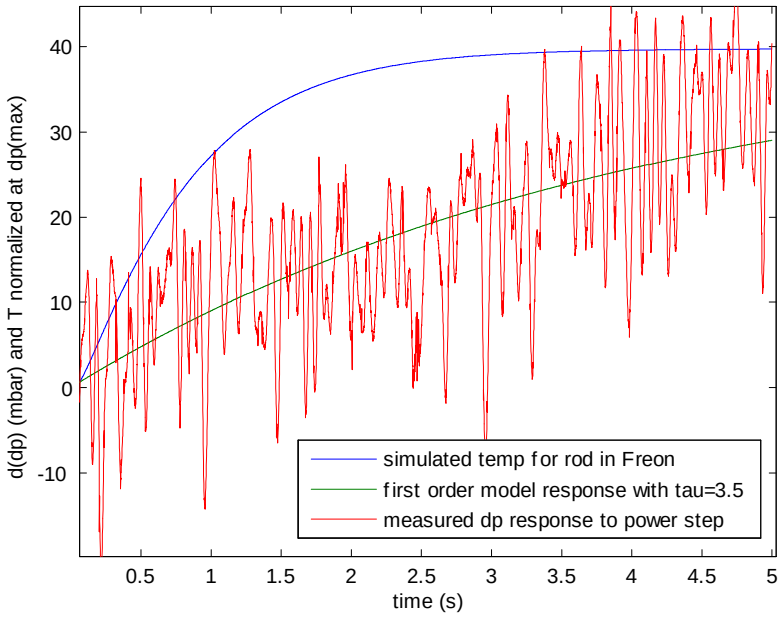

Figure 6.10: The dp response to a step in the power input, compared to the simulated model (scaled to $dp_{\max}$ for easy comparison) and a first order model with $\tau = 3,5\,\mathrm{s}$.

both gain and phase shift can produce valuable information about the heat transfer from the heating rods to the coolant. For a range of frequencies the following power input was applied:

$$P(t) = 25000 + 4000 \sin(2\pi f t) \tag{6.5}$$

The gain was obtained from the recorded figure (an example of such a graph for $f = 0.06\,\mathrm{Hz}$ is given in figure 6.11) by averaging the amplitudes of the pressure drop over the core and defining the gain to be unity at 85 mbar, since there is no simple relation between the input power and the pressure drop over the core. Nevertheless, the gain characteristic remains the same. The phase shift was obtained through the cross-correlation function in Matlab. The first maximum in these cross-correlation graphs equals the phase shift for the frequency in question.

Gain plots can be seen in figures 6.12 and 6.13, in which different second and first order models are compared to the data respectively.

Several remarks can be made about these figures. The data we does not necessarily seem to indicate a second order process. This becomes clear when we compare the data to several second order systems in figure 6.12. Especially for higher frequencies, the attenuation for second order systems is larger. A first order system attenuates less quickly. In figure 6.13 we can see the measurement data compared with some first order models. These models seem to fit the measurement data much better then the second order models. This leads us to the conclusion that the heat transfer process in Genesis can at least be approximated with a first order function, with a single time constant of 3,5 s. There is a number of options for explaining this:

- The $G_{dp,P}$ could simply be a first order function. This would be unexpected, but it could possibly be a good approximation, as is shown in figure 6.10.
- Secondly, the change in flow through the core might have had a bigger influence than expected. Although a pump was installed to prevent the flow from oscillating with the power input, it still does show an oscillation during measurements due to natural circulation (so there might be more physics to reckon with). This effect could have had a big influence on the pressure drop over the core, disturbing the gain measurements. This effect could explain (a part of) G_{add}.

It might have become clear that more data should be gathered for any of these options, to be able to conduct an effective curve fitting process in Matlab or Origin. Unfortunately, just after conducting these measurements, the Genesis facility broke down and additional measurements could not be taken for an indefinite period of time.

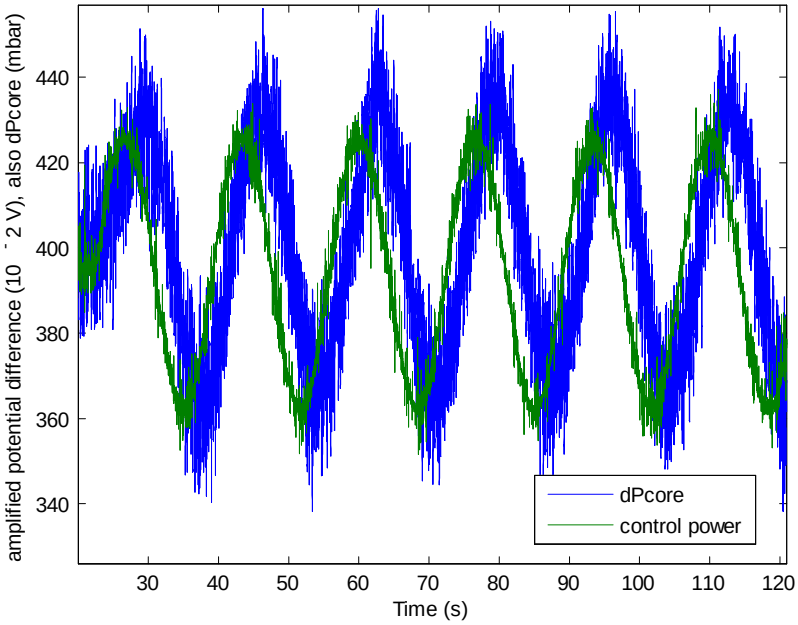

Figure 6.11: The computer control Voltage ($\times 10^{-2}$) compared to the pressure drop over the core for $f = 0,06\,\mathrm{Hz}$. The phase shift between both signal is clearly visible.

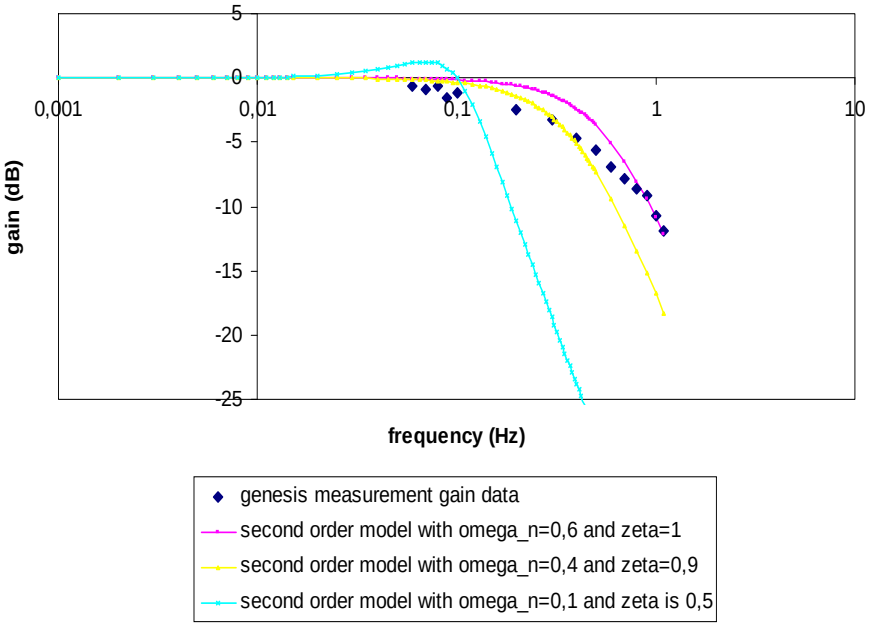

Figure 6.12: The measured gain for several input frequencies, compared with a second order model with a number of different parameters.

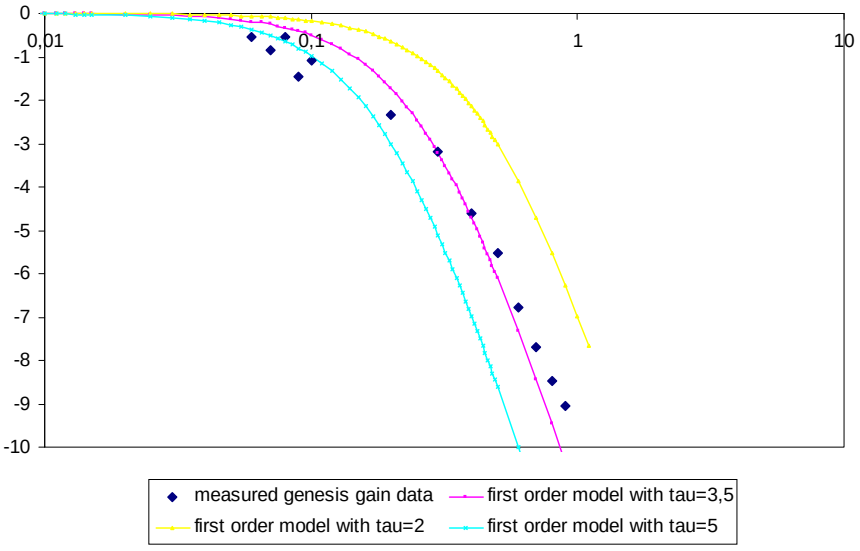

Figure 6.13: Measured gain in dB over a range of frequencies, compared to a first order model.

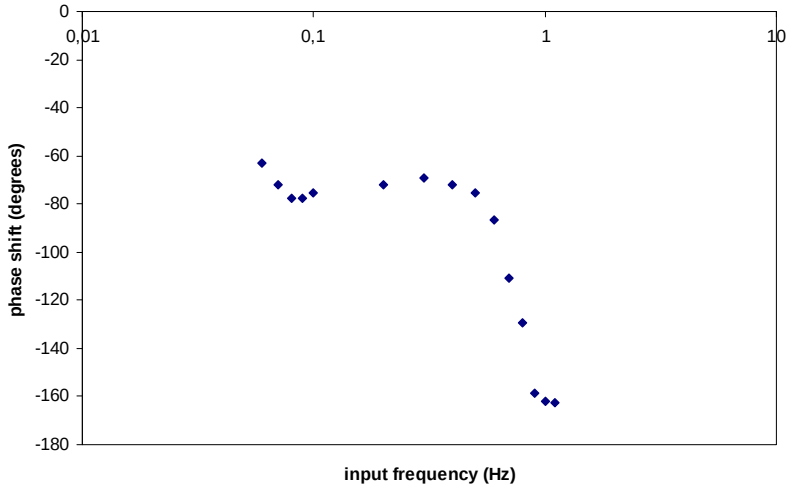

Figure 6.14: Phase shift of pressure drop over the core compared to the input power signal (in degrees).

After comparing the phase shift over a range of frequencies (shown figure 6.14) with figure 6.23 in Oppenheim and Willsky [13], we can conclude that the heat transfer does not have the characteristics of a first order nor of a second order system. However, for higher frequencies, the phase shift approaches -180 °. This is typical for a second order system. Still, for $f \longrightarrow 0$, the phase shift for a second order system should always go to zero. It can be concluded that more (complex) physics is invloved here.

If we do compare the measured phase shift to a second order system, we obtain the result shown in figure 6.15 .From figure 6.14, we concluded that the corner frequency ω_n would then turn out to be approximately 0,65 Hz.Now we can fit figure 6.14 with some second order models, keeping the corner frequency ω_n =0,65 Hz and varying the damping ratio ζ.

The models with $\zeta = 0,05$ and $\zeta = 0,1$ resemble the acquired data most. The value for ζ for the Genesis system, will be in between those two values. Again, we can see a discrepancy between the model and measurement data for lower frequencies. This could provide more evidence for the opinion that a higher order function is governing the heat transfer in Genesis and an extra transfer function G_{add} should be introduced.

6.8.5 Cross-correlation for Genesis oscillatory measurements

Another way to interpret the data is by means of the cross-correlation between the power input P and the pressure drop over the core dp in order

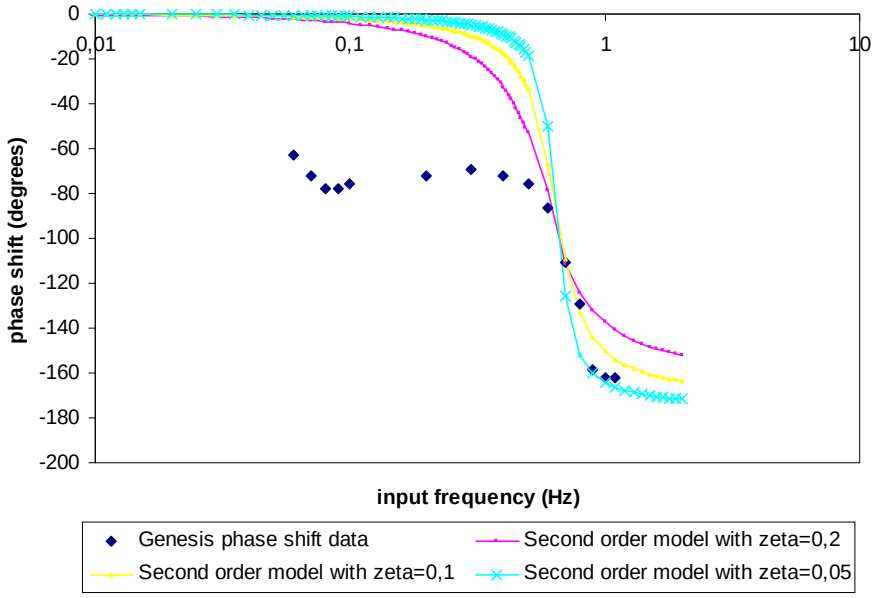

Figure 6.15: The phase shift, determined by oscillatory power input signals in Genesis, compared with a number of second order models (ω_n =0,65 Hz).

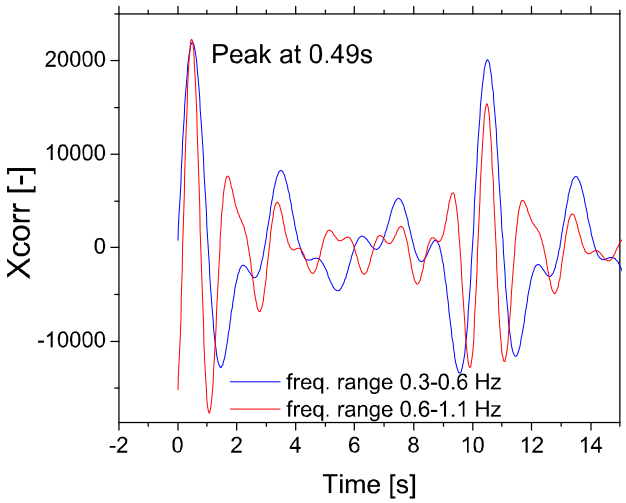

Figure 6.16: The cross-correlation of the power input signal P and the pressure drop over the core dp for a high and a low frequency range. A peak in the cross-correlation is clearly visible at $t = 0,49$ s.

to look for distinct delays of information. This can be done by using the cross-correlation function in Matlab. This has been done by Marcel [25] for the data provided by this experiment. The resulting cross-correlation for a high and a low frequency range can be found in figure 6.16. The cross-correlation is periodical due to cross-correlating multiple signals with different frequencies in one datafile, directly following one another.

A distinct peak is found at $t = 0,49$ s. This means that there is at least one component in the total Genesis transfer function $G_{dp,P}$, associated with this peak, that is quite fast. From the Genesis conditions during the oscillatory measurements, found in tables G.1 and G.2 in Appendix 7, the core inlet velocity v_0 and the traveling time for the core $t_{core,2\Phi}$ can be determined. Marcel [25] has found the values to be $v_0 = 1,48 \frac{\mathrm{m}}{\mathrm{s}}$ and $t_{core,2\Phi} = 0,28\,\mathrm{s}$. Furthermore, from Marcel [25], we know that the void traveling time through the riser above the core is in the order of three seconds[1], so the natural circulation effect cannot possibly be associated with the first peak, since the delay for this effect should be larger.

Based on this fact, the value for the traveling time through the core and

[1] The exact value calculated by Marcel [25] was $t_{riser} = 3,24$ s. However, this value is a result of slightly different Genesis conditions and, moreover, an unforced flow process. Nevertheless, there is no reason to believe that the value for t_{riser} will differ much.

the values for the time constants of the simulated transfer function for heat transfer to a Freon boundary layer ($\tau_1 = 0,12\,\mathrm{s}$ and $\tau_2 = 0,75\,\mathrm{s}$), we can explain the existence and position of the positive peak by the delays caused by the combined transfer function of the rod, the transfer function for the boundary layer and the transfer function for the vapor residence time in the core (schematically $G_{rod} \cdot G_{cool} \cdot G_{rt}$).

Unfortunately, while the cross-correlation analysis does seem to confirm the simulation of the heat transfer in Freon, it does not provide an explanation for the fact that the Genesis response to a step function is so much slower. In other words, we still do not have an expression for G_{add}, the extra transfer function caused by a thus far unknown effect. We try to find the solution for this problem by comparing the data to previous measurements of the Genesis total transfer function.

6.8.6 Comparison to other results for the Genesis transfer function

Within the Physics of Nuclear reactors group, more experiments have been conducted previously to find an expression for the total Genesis transfer function, i.e. $G_{dp,P}$. Marcel [25] conducted experiments by adding white noise to the power input signal and determining the cross-correlation between the input power P and the recorded pressure drop over the core dp. Since white noise should theoretically contain all frequencies, the response to all these frequencies can be determined at the same time. In practice the frequency range in the white noise is not infinite, but large enough to contain all frequencies in our region of interest. An important difference with the oscillatory measurements, is that the experiment by Marcel was not conducted with a forced flow, so no pump was used to regulate the flow. The obtained cross-correlation characteristic can be found in figure 6.17.

The cross-correlation of the measured data is compared to an estimated fourth order transfer function. It can be noted in figure 6.17 that a second peak was measured. The inlet velocity for the conditions during the experiment (found in table in Appendix 8) was found to be $v_0 = 1,00\frac{\mathrm{m}}{\mathrm{s}}$ and the core traveling time $t_{core,2\Phi} = 0,45\,\mathrm{s}$. Also, the void traveling time through the riser, above the core, was calculated $t_{riser} = 3,24\,\mathrm{s}$. Based on figure 6.17 and the two traveling times a number conclusions can be drawn:

- There are at least two different components present in the total Genesis transfer function $G_{dp,P}$; a fast component associated with the first sharp peak at $t = 0,67$ s and a slower component associated with the broader peak at around $t = 4,0$ s.
- The first peak is associated with $G_{rod} \cdot G_{cool} \cdot G_{rt}$ again. Thereby following the same reasoning as in section 6.8.5. The values for the

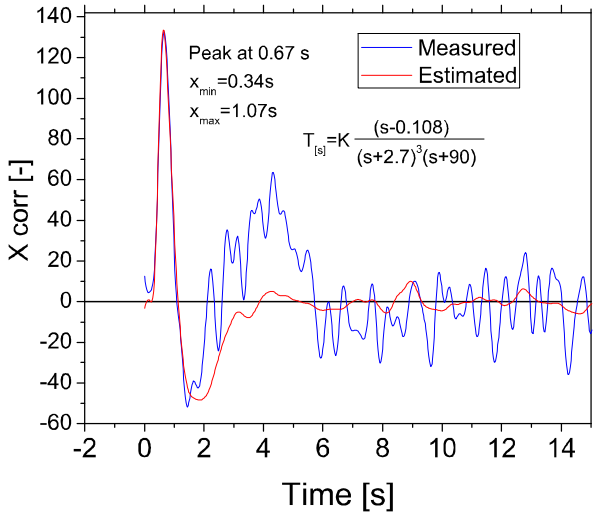

Figure 6.17: The cross-correlation of the power P and core pressure drop dp time series, compared to the best estimate transfer function.

time constants for the separate processes (for $G_{rod} \cdot G_{cool}$, $\tau_1 = 0,12\,\mathrm{s}$ and $\tau_2 = 0,75\,\mathrm{s}$ and $t_{core,2\Phi} = 0,45\,\mathrm{s}$) seem to support this conclusion.

- The negative peak that can be noticed in figure 6.17, is most likely associated with the decrease of the flow because of the initial increase of the friction due to void creation.

- Finally, since the time difference between the two positive peaks (about $3,3$ s) agrees very well with the calculated traveling time found for the riser section ($t_{riser} = 3,24\,\mathrm{s}$), it can be concluded that the second peak, or the slow component, is caused by a natural circulation effect. The extra void in the riser causes an increase in driving force for the natural circulation, by which the flow is increased. Most likely, this effect could be the cause of the slow response suggested in section 6.8.3 and was hence present in all measurements at the Genesis facility. In that case, the unknown additional transfer function G_{add} can be named G_{nc}; 'transfer function due to the natural circulation effect'. It also explains the deviation of the simulations from the step function measurements in figure 6.10; the response we are looking at in this figure is dominated by the (very slow) response of G_{nc} to a step function[2]. The effects

[2] Although the step function and the oscillatory experiments were conducted in forced

of the fast components disappear in the noise. Additional evidence to support this conclusion is the fact that the first order fit of the measured step response has a time constant of $3,5\,\mathrm{s}$, which corresponds quite well with the location of the second peak in figure 6.17. The large delay due to the natural circulation effect cannot be found in figure 6.16, although there seems to be a small peak near four seconds.

A transfer function was derived from figure 6.17 by Marcel [25] without taking the natural circulation effect into account. Since only the first peak in figure 6.17, relates to the transfer function caused by G_{rod}, G_{cool} and G_{rt}, the part of the total transfer function $G_{dp,P}$ in which we are mainly interested. The Bode plots of this estimated total transfer function can be found in figure 6.18. If we compare these diagrams to the gain and phase plots in figures 6.13 and 6.14, we notice that they are very different. This might be explained by the fact that G_{nc} has not been taken into account yet in the estimation, while they are, naturally, present in the measurements.

Since we are unable to find a complete expression for $G_{dp,P}$, G_{nc} and G_{rt}, we cannot single out an expression for G_{cool} either. If we decide that the simulations for the Genesis rod in Freon are reliable, naturally we could derive G_{cool} from the simulated $G_{cool} \cdot G_{rod}$ and the G_{rod} itself. However, it would be better if an experimental expression for $G_{cool} \cdot G_{rod}$ could be derived in future experiments to find a boundary layer transfer function that is in agreement with reality for sure.

flow conditions, quite a large power step (or power amplitude respectively) was applied to the input signals. The effect of the natural circulation can therefore not be neglected and will be present in both measurements.

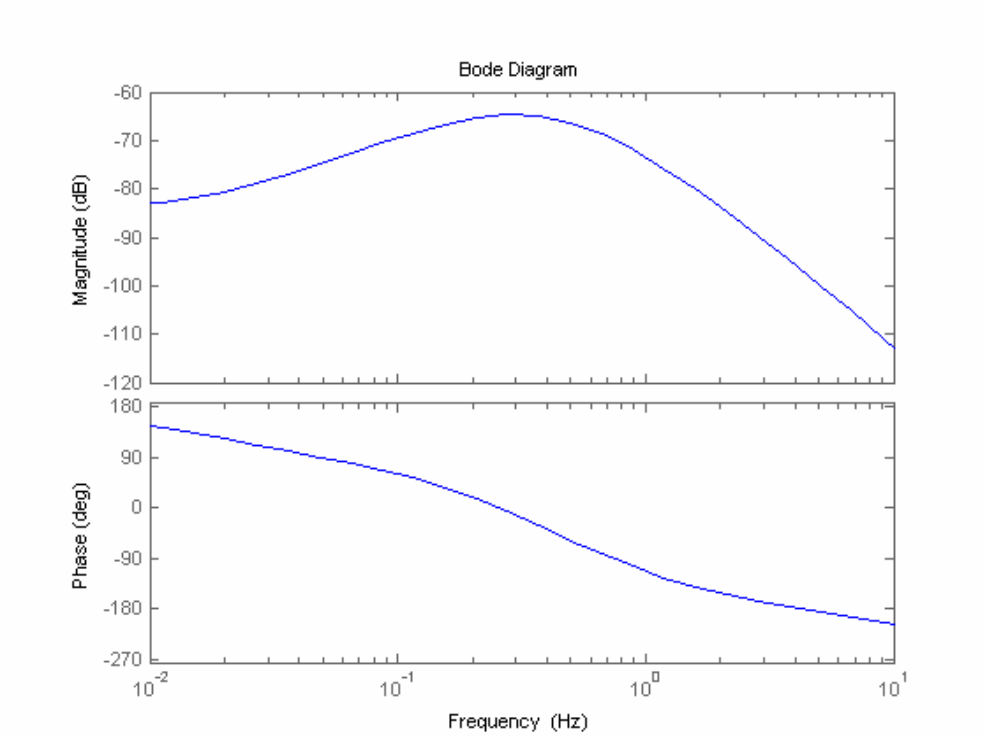

Figure 6.18: Bode plots for the estimated total transfer function $G_{dp,P}$, based on the white noise measurements.

7. Conclusions

7.1 Main conclusions

The simulations conducted for this experiment, have turned out to be a good approximation of reality. This can be derived from the fact that, after corrections for the local power increase and the thermocouple attachment method, the predicted course for the temperature development at the surface of the Genesis rod in air corresponds nicely with empirical data.

The transfer of heat through a single Genesis rod, turned out to be a second order process. The time constants for heat transfer through the rod only were found to be $0,03$ s and $0,28$ s by imposing the boundary condition $T(t) = T(0)$ and fitting the obtained curve in Origin. For a rod in the Genesis core, the time constants of the transfer function were determined to be $0,12$ s and $0,75$ s. These values indicate that the heat transfer from the rod surface to the coolant is slower than the heat transfer through the rod itself. However, the time constants are still of the same order, so the electrically heated rod in the Genesis facility are a not good approximation for the real, uranium rods, since the rod does have some influence on the heat transfer process.

Determining the gain and phase shift characteristics for harmonic input signals turned out to be unsuccessful. Judging by the gain characteristic the total Genesis response seems to be a first order function with a time constant of approximately $3,5$ s, while the phase shift characteristic clearly show that the total Genesis transfer function is nor first nor second order. From this it can be concluded that more physics plays a part in the transfer function, than can be incorporated in a first or second order model. To investigate further, the measurement data is re-interpreted by calculating the cross-correlation of the input signal P and the output signal dp. The cross-correlation results and comparison to previous measurements of the Genesis total transfer function characteristics, leads us to the conclusion that there is a slow (approximately $3,3$ s) and a fast component (approximately $0,5$ seconds) present in the total transfer function $G_{dp,P}$, both depending on the conditions for the Genesis facility during measurements. The slow component, identified as G_{nc}, the natural circulation transfer function, is caused by the traveling time of the created void through the riser section above the core and the fast component is associated with the heat transfer from the resistance wire to the coolant ($G_{rod} \cdot G_{cool}$) and the void traveling

time through the core. Also it becomes perfectly clear that $G_{dp,P}$ is a higher order system. An expression found in the literature that incorporates the core traveling time transfer function, but neglects G_{nc}, is already a fourth order function. Still, the gain and phase shift plots of this function do not match the gain and phase shift plots from the measurement data. This suggests that an even higher order function, incorporating G_{nc} is necessary to obtain a better fit.

We now also have an explanation for the disagreement of the simulated Genesis response to a step function and the corresponding measurement. The slow component G_{nc} is incorporated in the measured signal and due to the high noise ratio becomes the dominant trend.

Finally, a central problem for the interpretation of the Genesis measurements was the small amount of available data points. Unfortunately, no more data could be gathered due to a temporary breakdown of the Genesis facility.

7.2 Recommendations

I would recommend designing a method of determining the total transfer function $G_{dp.P}$, without introducing fluctuations in the flow through the core, if possible. Of course, minimizing these fluctuations will also do.

Finding an expression for the total transfer function that incorporates the natural circulation component, would prove useful. Using this expression, we can contruct bode plots and compare them to the gain and phase shift plots found for the oscillatory measurements. From this we can see if all physics is now captures in the model, or that perhaps even more processes should be taken into account for the model to agree with the measurement data.

Furthermore, it would be interesting to find out the cause for the fact that the second peak does not appear in the cross-correlation graph for the measurements under oscillatory conditions. Although a forced flow is implemented, the amplitude of the oscillations much larger than for the white noise measurements. This should give rise to a larger fluctuation in the flow and thus a larger secondary peak than under the white noise input conditions.

Finally, it would be useful to construct an experiment to find the transfer functions for the traveling time through the core G_{rt} and for the transfer function due to the natural circulation. If we know G_{rt} and G_{nc}, we could split up the total transfer function completely into all named separate components, including a separate expression for G_{cool}, which cannot be singled out from the data in this experiment.

Bibliography

[1] T.H.J.J. van der Hagen, *"Experimental and theoretical evidence for a short effective fuel time constant in a boiling water reactor" ,* Nuclear Technology 83(2) p.171-181, 1988.

[2] Fysische transportverschijnselen I, H.E.A. van den Akker en R.F. Mudde, Delft University Press, 2003

[3] *Heat and mass transfer*, Frank M. White, Addison Wesley Publishing company, ISBN 0-201-17099-X, p. 405

[4] *Correlation for boiling heat transfer in convection flow,* J.C.A.Chen, ISEC Process design Der. 5:322, 1966.

[5] *Algemene Instructie 35 "Temperatuurmeting"*, Natuurkundig Practicum, TU Delft.

[6] http://www.omega.com/temperature/Z/pdf/z021-032.pdf

[7] hier de informatie van de maker van het gebruikte thermokoppel invullen

[8] http://instrumentation-central.com/TechNotes/TypeKTableC.pdf

[9] *Demonstratieproeven over kookverschijnselen,* S.J.D. van Stralen, Nederlands Tijdschrift voor Natuurkunde, 28, januari 1962.

[10] *Practicum Fysische Transportverschijnselen, proefinstructie kookverschijnselen,* Natuurkundig Practicum, TU Delft.

[11] *Algemene Instructie 34 "Warmtetransport"*, Natuurkundig Practicum, TU Delft

[12] *The boiling point of water,* Thomsen, V., The Physics Teacher. 35, 1997, pp 98-99.

[13] *Signals and Systems,* Alan V. Oppenheim and Alan S. Willsky, second edition 1997, Prentice hall, p. 227 and p. 451-456

[14] *Numerical heat transfer and fluid flow,* Suhas V. Patankar, 1980, Taylor and Francis.

[15] dr. ir. Martin Rohde, Physics of Nuclear Reactors group, Delft University of Technology

[16] *Transport Phenomena Data Companion,* L.P.B.M. Janssen and M.M.C.G. Warmoeskerken, Delft University Press, third edition, 2001.

[17] *Thermal conductivity of R134a,* A. Leasecke, R.A. Perkins, C.A. Nieto de Castro, Fluid Phase equilibria, 80 (1992) 263-274.

[18] Dupont data sheet R134a. Enclosed in Appendix 4.

[19] *Transfer function of a system with sinusoidal input,* Don Johnson, Rice University, Texas, http://cnx.org

[20] Schriver, D.F. en M.A. Drezdzon, *The manipulation of air-sensitive compounds,* Second edition. Wiley & Sons (New York) 1986.

[21] *Binas, informatieboek havo-vwo voor het onderwijs in de natuurwetenschappen,* Vierde druk. Wolters-Noordhoff.1998.

[22] *Thermal conductivity of Magnesium Oxide from absolute, steady state measurements,* A.J. Slifka, B.J. Filla and J.M. Phelps, Journal of research of the National Institute of Standards and Technology, Volume 103, number 4, July0August 1998, p. 357.

[23] From personal communications with ing. A. Winkelman, Physics of nuclear reactors group, department of Radiation, Radionuclides & Reactors, Delft University of Technology.

[24] *Handbook of numerical heat transfer*, Minkowytz, Sparrow, Schneider and Hetcher, Wiley and Sons, ISBN: 0-471-83093-3.

[25] *Experimental determination of the power to dp_{core} transfer function,* Christian Marcel, Physics of Nuclear Reactors group, Delft University of technology.

A. Appendix 1: Uncertainty derivation

A.0.1 Antoine's relation

The uncertainty in Antoine's relation can be calculated as follows:

$$u(T_{antoine}) = \frac{3988,842}{(16,573 - \ln(p_v))^2 \cdot p_v} u(P_v) \tag{A.1}$$

Of course, the relation itself contains uncertainty too, since it is an empirical relation. It can be found in several different sources, but in this experiment the value given by Shriver [20] is used. The total uncertainty in the calculation of the boiling point using Antoine's relation now becomes:

$$(u(T_{boiling}))^2 = (u(T_{antoine}))^2 + (u(relation))^2 \tag{A.2}$$

In which $T_{boiling}$ is of course the calculated temperature for the boiling point.

B. Appendix 2: Equipment

A list of equipment used in the numerical model verification measurements.

- Agilent 33120A, 15 MHz function/arbitrary waveform generator.
- Fluke PM3380B, 100MHz Combiscope.
- Hatfield instruments, type 2105 analog attenuator.
- Canberra amplifier, incorporated in Genesis setup.
- National instruments DAQ/MX data input cards
- Delta elektronika power supply SM 300-5
- Digitale schuifmaat, Mitutoyo "Absolute Digimatic"

C. Appendix 3: Algorithm

In this appendix the simulation algorithm for a vertical rod in freon is given:

```
      program heatrod

      implicit none

      Double precision T(0:1001,2)
      Real lambda,rho,cp,dr,dt,q0
      Real lambda_mgo,rho_mgo,cp_mgo
      Real lambda_clad,rho_clad,cp_clad
      Real lambda_liq,rho_liq,rho_vap,cp_fre,visco_liq,visco_gas,hfg
      Real G,alfa
      Real Gr, Pr, Ra
      Real R_rod,R_mgo,R_clad,L_rod,r_heat_rod,dr_wire
      Real q,k,dump
      Double Precision dtdr(0:1001),d2tdr2(0:1001)
      Integer i,j,nt,nr,nr_mgo,n,i_heat,di_wire
      Real h_c,h_nb,h_tp,sigma

!     Rod properties
      R_mgo=0.263e-2
      R_clad=0.45e-3
      L_rod=1.41
      r_heat_rod=0.53*R_mgo
      dr_wire=3e-4

      q0=4000.0/(L_rod*3.14*
     &   ((r_heat_rod+0.5*dr_wire)**2-(r_heat_rod-0.5*dr_wire)**2))
      R_rod=R_mgo+R_clad

!     Properties of the MgO
      lambda_mgo=45.0
      rho_mgo=3580.0
      cp_mgo=877.0
```

C. Appendix 3: Algorithm

```
!     Properties of the cladding (Stainless steel)
      lambda_clad=14.2
      rho_clad=7800.0
      cp_clad=460.0

!     Properties of freon
      lambda_liq=0.00826
      rho_liq=1128.3
      rho_vap=59.49
      cp_fre =1525.0
      visco_liq=0.169e-3
      visco_gas=0.0124e-3
      hfg=158
      sigma=5.83e-3

!     Properties of genesis conditions
      G=442.0
 !     D=0.0010


!     Numerical quantities (dimensionless)
      nr=500
      dr=R_rod/nr
      dt=2.0e-7
      nt=int(5./dt)

!     Watch out! Th value for dt is not chosen at random. criterium:
!     (a*dt)/(dr**2).le.1/2


      i_heat=int(r_heat_rod/R_rod*nr)
      di_wire=int(dr_wire/R_rod*nr)
      nr_mgo=int(R_mgo/R_rod*nr)

      write(*,*) 'Power density = ',q0,' W/m^3'
      write(*,*) 'Number of time steps = ',nt
      write(*,*) 'Thickness heated wire = ',di_wire,' points'
      write(*,*) 'Number of MgO points = ',nr_mgo
      write(*,*) 'Number of cladding points = ',nr-nr_MgO
      read*

!     Initialize temperature in rod and cladding
      do i=0,nr
        do j=1,2
                T(i,j)=0.
                dtdr(i)=0
                d2tdr2(i)=0
        enddo
      enddo
```

C. Appendix 3: Algorithm

```
!     Open data file
      open(unit=1,file='ts.dat')
      open(unit=2,file='prof.dat')

!     Calculate transient rod temperature profile in the MgO
      do n=1,nt
        do i=1,nr_mgo-1
          lambda=lambda_mgo
          rho=rho_mgo
          cp=cp_mgo
          k=lambda/(rho*cp)

          if ((i.ge.(i_heat-di_wire/2)).and.
     &        (i.le.(i_heat+di_wire/2))) then
              q=q0

          else
            q=0.
          endif

          dtdr(i)=(T(i+1,1)-T(i-1,1))/(2.0*dr)
          d2tdr2(i)=(T(i+1,1)-2*T(i,1)+T(i-1,1))/dr**2.0

          T(i,2)=(k/(i*dr)*dtdr(i)+k*d2tdr2(i)+q/(rho*cp))*dt+T(i,1)

        enddo

!     We need to make a correction on the transition point between
!     the MgO and the cladding:

       dump=lambda_mgo/lambda_clad
        T(nr_mgo,2)=(dump*(T(nr_mgo-2,1)-4*T(nr_mgo-1,1))-
     &            4.*T(nr_mgo+1,1)+T(nr_mgo+2,1))/(-3-3*dump)

!     Now we can go on with the Calculation of the transient rod
!     temperature profile in the cladding.
        do i=nr_mgo+1,nr
          lambda=lambda_clad
          rho=rho_clad
          cp=cp_clad
          k=lambda/(rho*cp)

          dtdr(i)=(T(i+1,1)-T(i-1,1))/(2*dr)

          d2tdr2(i)=(T(i+1,1)-2*T(i,1)+T(i-1,1))/dr**2

          if (i.eq.nr) then
            if (T(nr,1).lt.0) T(nr,1)=0.0
```

C. Appendix 3: Algorithm

```
!     The heat transfer coefficient for the convective + nucleate boiling part
!     derived in the Maple sheet 'heat transfer coefficient freon.mw'

!           Convective part: averaged over the length of the core section
            h_c=527
!           Nucleate boiling part: dependent on the wall temperature
            h_nb=168*(T(nr,1))
!           Total heat transfer coefficient (following chen, both additive)
            h_tp=h_c+h_nb

            dtdr(i)=-h_tp/lambda_clad*T(nr,1)
            d2tdr2(i)=(2*T(i,1)-5*T(i-1,1)+4*T(i-2,1)-T(i-3,1))/dr**2

          end if

          T(i,2)=(k/(i*dr)*dtdr(i)+k*d2tdr2(i))*dt+T(i,1)

        enddo

        T(0,2)=T(1,2)

!       Collect and save transient temperature data to file:

        if (1.0*int(n/1000.).eq.(n/1000.)) then
                write(1,*) n*dt,T(nr,2),-lambda_clad*dtdr(nr)
     &          ,h_tp
        endif

!       Also, print the data to the screen:

        if (1.0*int(n/10000.).eq.(n/10000.)) then
                write(*,*) n*dt,T(nr,2),-lambda_clad*dtdr(nr),h_tp
        endif


        do i=0,nr
                T(i,1)=T(i,2)
        enddo

      enddo

!     Save temperature profile through the rod:

      do i=0,nr
              write(2,*) i*dr,T(i,2),dtdr(i),d2tdr2(i)
      enddo

      close(unit=2)
      close(unit=1)

      end
```

D. Appendix 4: Dupont R134a data sheet

DUPONT

Suva®
refrigerants

Physical Property Data for
Suva® 134a, Suva® 409A, Suva® MP39, Suva® MP66, Freon® 12, and Freon® 500

Property	Suva® 134a	Suva® MP39	Suva® MP66	Suva® 409A	Freon® 12	Freon® 500
Refrigerant Number	R-134a	R-401A	R-401B	R-409A	R-12	R-500
Replaces	R-12	R-12	R-12, R-500	R-12	N/A	N/A
Chemical Formula/ Composition	CH_2FCF_3	R22/R152a/R124 53/13/34 wt%	R22/R152a/R124 61/11/28 wt%	R22/R142b/R124 60/15/25 wt%	CCl_2F_2	R12/R152a 73.8/26.2 wt%
CAS Number	811-97-2	R22:75-45-6 R152a:75-37-6 R124:2837-89-0	R22:75-45-6 R152a:75-37-6 R124:2837-89-0	R22:75-45-6 R142b:75-68-3 R124:2837-89-0	75-71-8	R12:75-71-8 R152a:75-37-6
Molecular Weight	102.03	94.4	92.8	97.45	120.93	99.31
Boiling Point at 1 atm, °F (°C)	–15.7 (–26.5)	–27.3 (–33.0)	–30.4 (–34.7)	–29.6 (–34.2)	–21.62 (–29.79)	–28.3 (–33.5)
Liquid Density at 77°F (25°C), lb/ft^3 (kg/m^3)	75.02 (1210)	74.5 (1194)	74.4 (1193)	76 (1217)	81.84 (1311)	72.16 (1156)
Vapor Pressure of Satd. Liquid at 77°F (25°C), psia (kPa)	96 (661.9)	112.1 (772.9)	118.8 (819.2)	116.3 (801.6)	94.6 (652.1)	111.5 (768.8)
Heat Capacity of Liquid at 77°F (25°C), Btu/lb °F (kJ/kgK)	0.339 (1.42)	0.310 (1.3)	0.310 (1.3)	N/A	0.232 (0.971)	0.258 (1.08)
Heat Capacity of Vapor at 1 atm at 77°F (25°C), Btu/lb °F (kJ/kgK)	0.204 (0.854)	0.176 (0.737)	0.173 (0.724)	N/A	0.145 (0.617)	0.175 (0.733)
Thermal Conductivity of Liquid at 77°F (25°C), Btu/hr.ft °F (W/mK)	0.0478 (0.0824)	0.0517 (0.09)	0.0517 (0.09)	N/A (0.0697)	0.0405 (0.0743)	0.0432
Thermal Conductivity of Vapor at 1 atm (101.3 kPa), Btu/hr.ft°F (W/mK)	0.00836 (0.0145)	0.00688 (0.0119)	0.00688 (0.0119)	N/A	0.00557 (0.00958)	N/A
Critical Temperature, °F (°C)	213.9 (101.1)	226 (108)	223 (106)	224.6 (107)	233.6 (112)	221.9 (105.5)
Critical Pressure, psia (kPa)	588.9 (4060)	668 (4604)	679 (4682)	667.2 (4600)	596.9 (4116)	641.9 (4426)
AEL/TLV, 8- or 12-hr TWA, ppm	1,000	1,000	1,000	1,000	1,000	1,000
ODP, CFC-12=1	0	0.03	0.035	0.05	1	0.738
GWP, CO2=1	1,300	973	1,062	1,288	8,500	6,310
ASHRAE Safety Classification	A1	A1/A1	A1/A1	A1/A1	A1	A1/A1
Refrigerant Cylinder Color, PMS Code	2975	177	124	465	White	109
Refrigerant Number	R-134a	R-401A	R-401B	R-409A	R-12	R-500

E. Appendix 5: Curve fitting information

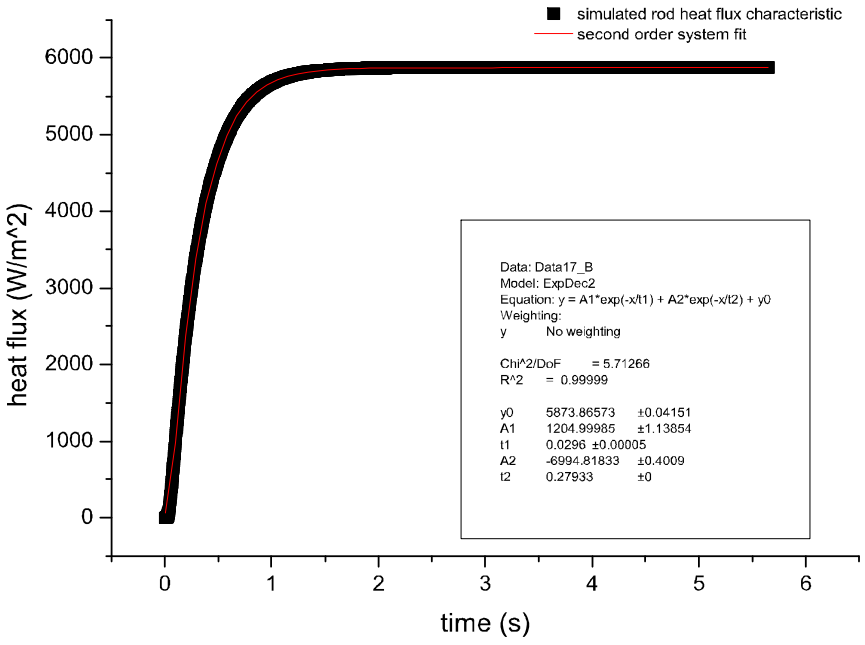

Simulated rod response to a step in the input power, fitted with a first order system.

E. Appendix 5: Curve fitting information

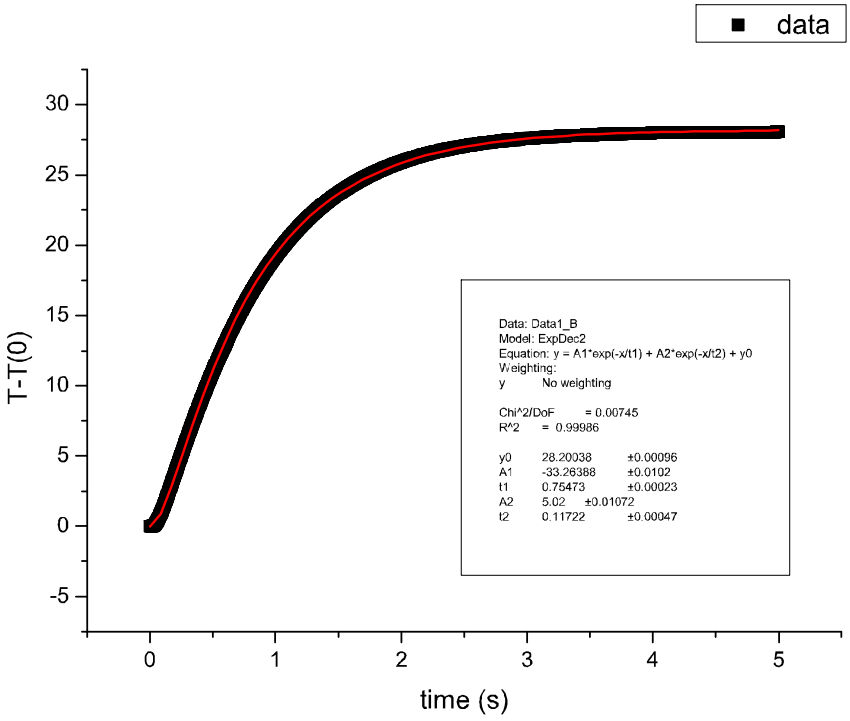

Figure E.1: The simulated heat flux data of vertically suspended rod in a (saturated) boiling freon environment, fitted with a second order system (red line).

F. Appendix 6: System Parameters used for the determination of h_{NB} and h_c

ρ_g	$56{,}49 \frac{\mathrm{kg}}{\mathrm{m}^3}$
ρf	$1128{,}3 \frac{\mathrm{kg}}{\mathrm{m}^3}$
c_p	$1525 \frac{\mathrm{J}}{\mathrm{kg\,K}}$
μ_f	$0{,}169 \times 10^{-3} (\mathrm{Pa\,s})$
μ_g	$0.0124 \times 10^{-3} (\mathrm{Pa\,s})$
λ_f	0,00826 $(\frac{\mathrm{W}}{\mathrm{m\,K}})$
D_e	0,00615 (m)
σ	$5{,}83 \times 10^{-3} (\frac{\mathrm{N}}{\mathrm{m}})$
h_{fg}	158 $(\frac{\mathrm{kJ}}{\mathrm{kg}})$
G	442 $(\frac{\mathrm{kg}}{\mathrm{m}^2\,\mathrm{s}})$

G. Appendix 7: Measures and conditions of the Genesis facility for oscillatory measurements

Table G.1: Measures of the Genesis facility

GENESIS	Units	Value
Core length	m	1,41
Riser length	m	6,02
Core area	m^2	$5{,}495 \cdot 10^{-4}$
Riser area	m^2	$13{,}9 \cdot 10^{-4}$
Liquid density	$\frac{kg}{m^3}$	1128,3
Latent heat	$\frac{kJ}{kg}$	158,39

Table G.2: Conditions in the Genesis facility at the time of the oscillatory measurements

N_{Zu}	3.25
N_{Sub}	$1, 2$
M	$0, 92 \frac{kg}{s} (\pm 1\%)$
Mean Power level	$25, 0\,kW$
Power sinusoidal amplitude	$\pm 16\%$
Forced circulation flow	

G. Appendix 7: Measures and conditions of the Genesis facility for oscillatory measurements

Table G.3: Conditions in the Genesis facility for the white noise measurements conducted by Marcel

N_{Zu}	$4, 9$
N_{Sub}	$1, 2$
M	$0, 62 \pm 10\% \frac{\mathrm{kg}}{\mathrm{s}}$
Mean Power level	$25, 3\,\mathrm{kW}$
Power noise level	$\pm 6\%$
Power noise cutoff frequency	$20\,\mathrm{Hz}$
Natural circulation flow	